Figure 4. Lfng regulates the amount of Notch signaling, which is critical for the determination of T-cell fate. (A) Transcripts of the *Lfng* gene in LK-FL cells (E15.5), derived from WT or Lfng-deficient mice (LfngKO), and in N1/3T3 were detected by real-time RT-PCR as described in the *Materials and methods*. Relative mRNA levels of the *Lfng* gene (Lfng relative expression ± SD) were calculated from the ratio of Lfng and 18S ribosomal RNA. (B) Lfng differentially modulates the amount of Notch signaling from ligands. Notch signaling in N1/3T3 or transfectants expressing both Notch1 and Lfng (Lfng-N1/3T3) induced by Dll4 or Jagged transfectants (positive, +; high positive, ++; below the panel) were analyzed by reporter assays as described in Fig. 1C. Data are representative of three independent experiments. (C) Jagged2 expressed at high levels on transfectants transduces an amount of Notch signaling similar to that induced by Dll4 in LK-FL cells. The quantity of transcripts of the *Hes1* gene in fresh LK-FL cells (pre) or in LK-FL cells cultured for 24 h on transfectants (below the panel) were evaluated by real-time RT-PCR as described in (A).

mice exhibit a pan-Notch defective phenotype and die at E11.5 [27–29]. However, the part(s) of the intracellular region of the ligands required for their association with Mib1 has still to be clarified, and there is no homologous sequence of amino acids when the intracellular regions of the Dll and Jagged families are compared. Thus, the functional role of these regions in signal transduction at the molecular level remains poorly understood. In this study, we showed that these regions were interchangeable between Dll4 and Jagged1 and that the chimeric molecules could induce Notch signaling. This result suggested that the two intracellular regions of Dll4 and Jagged1 function independently

of the extracellular region of the ligands and share the molecular machinery necessary to induce Notch signaling.

Jagged2 was also reported to support the development of HPC into NK cells on OP9 stromal cells in the presence of IL7, Flt3L and IL2 [30]. In contrast, Jagged1 supports NK-cell development only from DN thymocytes [13]. We detected a substantial NK1.1$^+$ population in the culture with Jagged2 stromal cells and the above cytokines, but NK1.1$^-$Thy-1$^+$ T-lineage cells clearly appeared (data not shown). Jagged1 did not have any effect on NK-cell induction under these conditions (data not shown). Transient or reduced Notch signaling was suitable for NK-cell induction on monolayer culture with stromal cells [31–33]. Thus, OP9 cells expressing Jagged2 as used in the previous study might transduce Notch signaling that is too weak for T-cell induction but is sufficient for NK-cell induction. However, it was not clear how stromal cells could express Jagged2 on the cell surface and trigger Notch signaling.

In this study, we first demonstrated that Notch signaling events mediated by Dll4 and Jagged2 were up- or down-regulated, respectively, by Lfng. Taken together with the results of earlier studies of Dll1 and Jagged1 [22, 34], it was clearly shown that the functional regulation by Lfng affected all ligands within the Dll and Jagged families. However, the inhibitory effect of Lfng on Jagged2-mediated signaling was remarkably less than the effect on Jagged1-mediated signaling. Thus, the signaling event(s) induced by Jagged2 may be resistant to Fringe-mediated modification of the Notch receptor, compared with signaling induced by Jagged1, and therefore Jagged2 retains the potential for T-cell induction from HPC that abundantly express Lfng.

In addition to Lfng, Manic fringe (Mfng) and Radical fringe were reported to have the same activity as glycosyltransferases in mammals, but Radical fringe did not suppress Jagged1-mediated Notch signaling *in vitro* [34]. We detected transcripts of the *Mfng* gene in LK-FL cells and demonstrated that Mfng as well as Lfng modified Notch signaling. We could see a decrease in T-cell induction upon culture of Lfng-deficient HPC on stromal cells expressing Dll4, but not the appearance of T-lineage cells from those cultured on stromal cells expressing Jagged1 (data not shown). We considered that Mfng compensated for the defect of Lfng in HPC during these cultures. Recent reviews described that Lfng$^{-/-}$, Mfng$^{-/-}$ HPC differentiated into T-lineage cells with Jagged1-mediated Notch signaling [35, 36]. This supported our speculation, but the details still need to be clarified.

We suggest in this study that within the extracellular region of Jagged2, the DSL domain primarily determines the magnitude of the signaling induced, independently of other extracellular regions, but the DSL domain is not engaged in the response to fringe-modified Notch. The latter seemed to be associated with the total structure of the extracellular region of the Jagged family, which is composed of at least the eight EGF-like repeats present in the shortened Jagged1 examined here. In addition, the Jagged1-based variant containing the DSL domain of Dll4 lost the Dll4 ability to induce signaling in N1/3T3 cells, but did not gain the activity to induce signaling in Lfng-N1/3T3 cells. To understand this phenomenon precisely, further examination is needed.
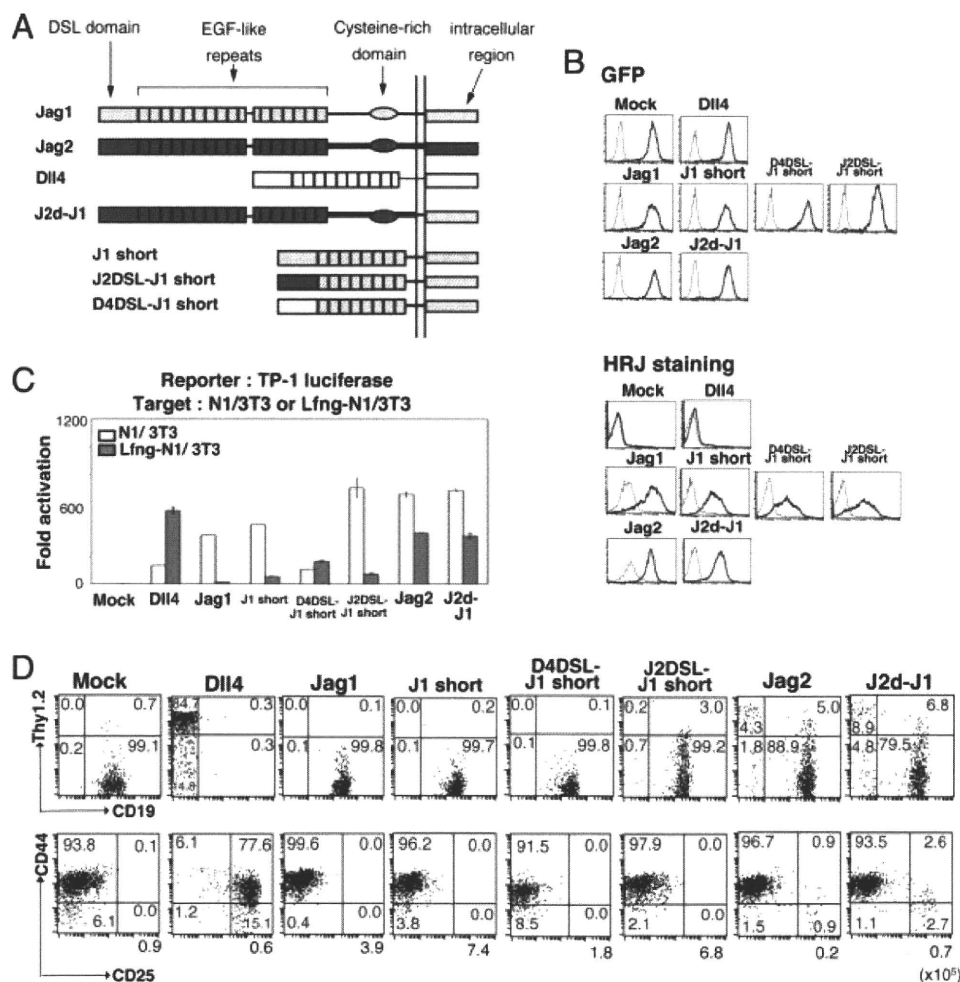
Figure 5. The DSL domain does not determine the T-cell induction function of individual Notch ligands. (A) Schematic structure of Dll4, Jagged 1 and Jagged-based variants. Dll4 and Jagged1, intact NotchL; J1 short, Jagged1-based variant with eight EGF repeats (identical to the Dll family) and missing the cysteine-rich domain; D4DSL-J1 short and J2DSL-J1 short, J1 short-based variants whose DSL domain is that of Dll4 or Jagged2, respectively. The DSL domain, EGF-like repeats and intracellular region of Jagged1 and Jagged2 are indicated by light-gray and dark-gray rectangles, respectively, and those of Dll4 are represented by open rectangles. The ovals indicate the cysteine-rich domain of Jagged family members. The transmembrane regions of Jagged1, Jagged2 and Dll4 are indicated by medium, bold and thin lines, respectively. (B) Flow cytometric analysis of various transfectants expressing intact Jagged1 or Jagged1-based variants with HRJ1-15 mAb (HRJ staining, lower panels) as described in Fig. 3B. Expression of GFP was also monitored (GFP, upper panels). (C) Notch signaling from Jagged1-based variants. Notch signaling in N1/3T3 or Lfng-N1/3T3 induced by Jagged1-based ligands or intact NotchL was analyzed by luciferase reporter assays as described in Fig. 1C. Data are representative of three independent experiments. (D) None of the Jagged1-based variants induced T-cell development *in vitro*. The experimental procedure is described in Fig. 2A.

These were the first data to show that a part of the extracellular region separately contributes to individual variations of NotchL activity, which is significant for understanding the features of the inter-molecular binding of NotchL and Notch.

T-cell induction *via* Jagged2 depended precisely on the density of the ligand on the cell surface. This directly demonstrated using intact NotchL on the cell surface that there is a certain threshold in Notch signaling for T-cell induction. This may be consistent with the previous findings that Notch signaling induced by immobilized Dll1 protein at high density, but not low density, was enough for T-cell induction [37, 38], and that T-cell induction on Dll1/OP9 was suppressed by the addition of γ-secretase inhibitor in a dose-dependent manner [39]. We showed here that each NotchL possesses potential to induce different magnitudes of signaling in

HPC, and differently supports T lymphopoiesis *in vitro* regardless of whether the NotchL is of the Dll or Jagged family. These differences within NotchL seem to be critical for the unique potential of individual ligands for neurogenesis [40], the regulation of immune responses [41, 42] and tumorigenesis [43].

Materials and methods

Plasmids and constructs

cDNA for murine Jagged1, Jagged2, Dll1 and Dll4 were kind gifts from Drs. S. Chiba (University of Tokyo, Tokyo, Japan), and

C. Mailhos (UCL, London, UK), respectively. To design the mutants lacking the intracellular region of Jagged1 or Dll4, called J1d or D4d, Jagged1 and Dll4 cDNA were truncated by insertion of a termination codon after Val (1093rd aa for Jagged1 and 657th aa for Dll4), by PCR with appropriate primers. For J1d-D4, which encoded the chimeric molecule of J1d and the intracellular region of Dll4 with two extra aa (His and Met) at the NdeI site, the cDNA for the intracellular region of Dll4 was also amplified by PCR with an NdeI site at the 5′ end and cloned into an additional NdeI site designed at the 3′ end of the J1d construct. To generate a cDNA for D4d-J1, the extracellular domain of Dll4 and the intracellular domain of Jagged1 were amplified by PCR with primers for reverse directions, and the amplified DNA was self-ligated to exclude the junction between D4d and the intracellular region of Jagged1. The cDNA of J2d-J1 was made by PCR. The full-length Jagged2 was inserted in front of a Jagged1 fragment missing the majority of the extracellular domain (Met; 1st aa through Ile; 1036th aa). The extracellular domain of Jagged2 and the intracellular domain of Jagged1 were amplified by PCR with primers for reverse directions and self-ligated to eliminate the intracellular domain of Jagged2 and the remaining sequence of the extracellular domain of Jagged1. For J1 short, Jagged1 was truncated deleting the sequence between nucleotide numbers 1584 and 3201 corresponding to amino acids Cys (529th aa) through Asp (1067th aa) by PCR with appropriate primers. For D4DSL-J1short and J2DSL-J1 short, we used the In-Fusion Dry-Down PCR Cloning Kit (Clontech Laboratories, Mountain View, CA). According to the manufacturer's method, the DSL domains of Dll4 (Val; 278th aa through Cys; 322th aa) or Jagged2 (Val; 196th aa through Cys; 240th aa) were fused with the J1 short cassette lacking the DSL domain (Val; 185th aa through Cys; 229th aa), respectively. All cDNA and variants for NotchL were cloned into the MIGR1 retrovirus vector.

Establishment of NIH-3T3 cells expressing NotchL

For establishment of NIH-3T3 cell lines expressing intact NotchL or their variants, retroviruses encoding NotchL and mutants were obtained after transfection into the Plat-E ecotropic packaging cell line as described previously [8]. Retrovirus-infected cells were collected 48 h after the infection and analyzed for GFP expression by flow cytometry. GFP-positive and -highly positive cells were obtained by sorting using a JSAN automatic cell sorter (Bay Bioscience, Kobe, Japan), giving rise to a >99% pure population as determined by post-sort analysis. Expression of Notch ligands or chimeric molecules on the cell surface was detected by staining with biotinylated anti-Jagged1, Jagged2, Dll1 or Dll4 mAb as described previously [44]. An isotype control of biotinylated hamster IgG was purchased from BD Biosciences (San Jose, CA).

Transient reporter assay

Reporter assays were carried out by the transient transfection of reporter plasmids TP1-luciferase (pGa981-6, including six copies

of RBPJk binding sites, constructed by Dr. L. Strobl [20]) and pRL-TK (Promega, Madison, WI) into N1/3T3, which was established as a stable transfectant with pTracer™-CMV (Invitrogen, Carlsbad, CA) encoding mouse Notch1. Each reporter plasmid (0.38 µg) was cotransfected into 5×10^4 cells in 24-well plates by a liposome-based method (Transfast, Promega) according to the manufacturer's instructions. Following 24-h culture after transfection, target cells were detached by trypsinization and co-cultured with stimulators (5×10^4, NIH-3T3 cells expressing NotchL) for 40 h. Cell lysates from the mixtures of two kinds of cells were then used for the luciferase assay. Lfng-N1/3T3 was generated by the infection of retroviruses encoding Lfng.

Antibodies and flow cytometry

Biotinylated TER-119, CD19 (MB19-1), CD11b (M1/70), GR-1 (RB6-8C5), PE-conjugated c-kit (2B8), Thy1.2 (53-2.1) and APC-conjugated CD19 (MB19-1) were all purchased from eBioscience (Mountain View, CA). HRJ1-5 was established by immunization of Armenian hamsters with a recombinant rat Jagged1-human Fc chimeric protein (R&D Systems, Minneapolis, MN). Expression of cell surface markers was analyzed by flow cytometry with a FACSCalibur (BD Biosciences).

Co-culture assay with stromal cells

In vitro cultures of LK-FL cells with stromal cells were described previously [8]. Briefly, lineage markers-(Lin; TER119, CD19, Mac-1, Gr-1) negative, c-kit-positive cells were isolated from E15.5 embryos and plated at 2×10^4 cells on a monolayer of stromal NIH-3T3-derived transfectants prepared in six-well culture dishes for 1 wk in the presence of 10 ng/mL recombinant IL7 (Peprotech, London, UK). For the culture of DP cells, PA6-derived transfectants were harvested in six-well culture dishes, and 2×10^4 LK-FL cells were cocultured for 14 days with 1 ng/mL IL7 and 5 ng/mL fms-like tyrosine kinase 3 ligand (Flt3L; Peprotech). After culture, growing cells were collected and analyzed for surface markers by flow cytometry. All mouse experiments were approved by the Animal Experimentation Committee (Tokai University, Isehara, Japan).

Quantitative reverse transcriptase-PCR

CD45-positive hematopoietic cells were harvested and purified from the co-cultures of LK-FL cells with NIH-3T3 expressing various NotchL at 24 h by AutoMACS. Total RNA was extracted with an RNeasy kit (Qiagen, Hilden, Germany) and transcribed with SuperScript III (Invitrogen). Quantitative PCR for the Hes1 gene was performed using TaqMan® Gene Expression Assays (Applied Biosystems, Foster City, CA).

References

1 Artavanis-Tsakonas, S., Rand, M. D. and Lake, R. J., Notch signaling: cell fate control and signal integration in development. *Science* 1999. **284**: 770–776.

2 Jundt, F., Anagnostopoulos, I., Foster, R., Mathas, S., Stein, H. and Dorken, B., Activated Notch1 signaling promotes tumor cell proliferation and survival in Hodgkin and anaplastic large cell lymphoma. *Blood* 2002. **99**: 3398–3403.

3 Sade, H., Krishna, S. and Sarin, A., The anti-apoptotic effect of Notch-1 requires p56lck-dependent, Akt/PKB-mediated signaling in T cells. *J. Biol. Chem.* 2004. **279**: 2937–2944.

4 Rangarajan, A., Talora, C., Okuyama, R., Nicolas, M., Mammucari, C., Oh, H., Aster, J. C. et al., Notch signaling is a direct determinant of keratinocyte growth arrest and entry into differentiation. *EMBO J.* 2001. **20**: 3427–3436.

5 Radtke, F., Wilson, A., Stark, G., Bauer, M., van Meerwijk, J., MacDonald, H. R. and Aguet, M., Deficient T cell fate specification in mice with an induced inactivation of Notch1. *Immunity* 1999. **10**: 547–558.

6 Han, H., Tanigaki, K., Yamamoto, N., Kuroda, K., Yoshimoto, M., Nakahata, T., Ikuta, K. and Honjo, T., Inducible gene knockout of transcription factor recombination signal binding protein-J reveals its essential role in T versus B lineage decision. *Int. Immunol.* 2002. **14**: 637–645.

7 Pui, J. C., Allman, D., Xu, L., DeRocco, S., Karnell, F. G., Bakkour, S., Lee, J. Y. et al., Notch1 expression in early lymphopoiesis influences B versus T lineage determination. *Immunity* 1999. **11**: 299–308.

8 Hozumi, K., Abe, N., Chiba, S., Hirai, H. and Habu, S., Active form of Notch members can enforce T lymphopoiesis on lymphoid progenitors in the monolayer culture specific for B cell development. *J. Immunol.* 2003. **170**: 4973–4979.

9 Schmitt, T. M. and Zúñiga-Pflücker, J. C., Induction of T cell development from hematopoietic progenitor cells by delta-like-1 in vitro. *Immunity* 2002. **17**: 749–756.

10 Hozumi, K., Negishi, N., Suzuki, D., Abe, N., Sotomaru, Y., Tamaoki, N., Mailhos, C. et al., Delta-like 1 is necessary for the generation of marginal zone B cells but not T cells in vivo. *Nat. Immunol.* 2004. **5**: 638–644.

11 Hozumi, K., Mailhos, C., Negishi, N., Hirano, K., Yahata, T., Ando, K., Zuklys, S. et al., Delta-like 4 is indispensable in thymic environment specific for T cell development. *J. Exp. Med.* 2008. **205**: 2507–2513.

12 Jaleco, A. C., Neves, H., Hooijberg, E., Gameiro, P., Clode, N., Haury, M., Henrique, D. and Parreira, L., Differential effects of Notch ligands Delta-1 and Jagged-1 in human lymphoid differentiation. *J. Exp. Med.* 2001. **194**: 991–1002.

13 Lehar, S. M., Dooley, J., Farr, A. G. and Bevan, M. J., Notch ligands Delta 1 and Jagged1 transmit distinct signals to T-cell precursors. *Blood* 2005. **105**: 1440–1447.

14 Calvi, L. M., Adams, G. B., Weibrecht, K. W., Weber, J. M., Olson, D. P., Knight, M. C., Martin, R. P. et al., Osteoblastic cells regulate the haematopoietic stem cell niche. *Nature* 2003. **425**: 841–846.

15 Koch, U., Lacombe, T. A., Holland, D., Bowman, J. L., Cohen, B. L., Egan, S. E. and Guidos, C. J., Subversion of the T/B lineage decision in the thymus by lunatic fringe-mediated inhibition of Notch-1. *Immunity* 2001. **15**: 225–236.

16 Tan, J. B., Visan, I., Yuan, J. S. and Guidos, C. J., Requirement for Notch1 signals at sequential early stages of intrathymic T cell development. *Nat. Immunol.* 2005. **6**: 671–679.

17 Visan, I., Tan, J. B., Yuan, J. S., Harper, J. A., Koch, U. and Guidos, C. J., Regulation of T lymphopoiesis by Notch1 and Lunatic fringe-mediated competition for intrathymic niches. *Nat. Immunol.* 2006. **7**: 634–643.

18 Tsukumo, S., Hirose, K., Maekawa, Y., Kishihara, K. and Yasutomo, K., Lunatic fringe controls T cell differentiation through modulating notch signaling. *J. Immunol.* 2006. **177**: 8365–8371.

19 Moriyama, Y., Sekine, C., Koyanagi, A., Koyama, N., Ogata, H., Chiba, S., Hirose, S. et al., Delta-like 1 is essential for the maintenance of marginal zone B cells in normal mice but not in autoimmune mice. *Int. Immunol.* 2008. **20**: 763–773.

20 Minoguchi, S., Taniguchi, Y., Kato, H., Okazaki, T., Strobl, L. J., Zimber-Strobl, U., Bornkamm, G. W. and Honjo, T., RBP-L, a transcription factor related to RBP-Jkappa. *Mol. Cell Biol.* 1997. **17**: 2679–2687.

21 Sun, X. and Artavanis-Tsakonas, S., The intracellular deletions of Delta and Serrate define dominant negative forms of the Drosophila Notch ligands. *Development* 1996. **122**: 2465–2474.

22 Hicks, C., Johnston, S. H., di Sibio, G., Collazo, A., Vogt, T. F. and Weinmaster, G., Fringe differentially modulates Jagged1 and Delta1 signalling through Notch1 and Notch2. *Nat. Cell Biol.* 2000. **2**: 515–520.

23 Shimizu, K., Chiba, S., Saito, T., Takahashi, T., Kumano, K., Hamada, Y. and Hirai, H., Integrity of intracellular domain of Notch ligand is indispensable for cleavage required for release of the Notch2 intracellular domain. *EMBO J.* 2002. **21**: 294–302.

24 Wang, W. and Struhl, G., Distinct roles for Mind bomb, Neuralized and Epsin in mediating DSL endocytosis and signaling in Drosophila. *Development* 2005.**132**: 2883–2894.

25 Le Borgne, R., Remaud, S., Hamel, S. and Schweisguth, F., Two distinct E3 ubiquitin ligases have complementary functions in the regulation of delta and serrate signaling in Drosophila. *PLoS Biol.* 2005. **3**: e96.

26 Lai, E. C., Roegiers, F., Qin, X., Jan, Y. N. and Rubin, G. M., The ubiquitin ligase Drosophila Mind bomb promotes Notch signaling by regulating the localization and activity of Serrate and Delta. *Development* 2005. **132**: 2319–2332

27 Koo, B. K., Lim, H. S., Song, R., Yoon, M. J., Yoon, K. J., Moon, J. S., Kim, Y. W. et al., Mind bomb 1 is essential for generating functional Notch ligands to activate Notch. *Development* 2005. **132**: 3459–3470

28 Koo, B. K., Yoon, M. J., Yoon, K. J., Im, S. K., Kim, Y. Y., Kim, C. H., Suh, P. G. et al., An obligatory role of mind bomb-1 in notch signaling of mammalian development. *PLoS ONE* 2007. **11**: e1221.

29 Barsi, J. C., Rajendra, R., Wu, J. I. and Artzt, K., Mind bomb1 is a ubiquitin ligase essential for mouse embryonic development and Notch signaling. *Mech. Dev.* 2005. **122**: 1106–1117.

30 DeHart, S. L., Heikens, M. J. and Tsai, S., Jagged2 promotes the development of natural killer cells and the establishment of functional natural killer cell lines. *Blood* 2005. **105**: 3521–3527.

31 Carotta, S., Brady, J., Wu, L. and Nutt, S. L., Transient Notch signaling induces NK cell potential in Pax5-deficient pro-B cells. *Eur. J. Immunol.* 2006. **36**: 3294–3304.

32 Rolink, A. G., Balciunaite, G., Demolière, C. and Ceredig, R., The potential involvement of Notch signaling in NK cell development. *Immunol. Lett.* 2006. **107**: 50–57.

33 De Smedt, M., Hoebeke, I., Reynvoet, K., Leclercq, G. and Plum, J., Different thresholds of Notch signaling bias human precursor cells toward B-, NK-, monocytic/dendritic-, or T-cell lineage in thymus microenvironment. *Blood* 2005. **106**: 3498–3506.

34 Yang, L. T., Nichols, J. T., Yao, C., Manilay, J. O., Robey, E. A. and Weinmaster, G., Fringe glycosyltransferases differentially modulate Notch1 proteolysis induced by Delta1 and Jagged1. *Mol. Biol. Cell* 2005. **16**: 927–942.

35 Stanley, P. and Guidos, C. J., Regulation of Notch signaling during T- and B-cell development by O-fucose glycans. *Immunol. Rev.* 2009. **230**: 201–215.

36 Yuan, J. S., Kousis, P. C., Suliman, S., Visan, I. and Guidos, C. J., Functions of notch signaling in the immune system: consensus and controversies. *Annu. Rev. Immunol.* 2010. **28**: 343–365.

37 Dallas, M. H., Varnum-Finney, B., Delaney, C., Kato, K. and Bernstein, I. D., Density of the Notch ligand Delta1 determines generation of B and T cell precursors from hematopoietic stem cells. *J. Exp. Med.* 2005. **201**: 1361–1366.

38 Delaney, C., Varnum-Finney, B., Aoyama, K., Brashem-Stein, C. and Bernstein, I. D., Dose-dependent effects of the Notch ligand Delta1 on ex vivo differentiation and in vivo marrow repopulating ability of cord blood cells. *Blood* 2005. **106**: 2693–2699.

39 Schmitt, T. M., Ciofani, M., Petrie, H. T. and Zúñiga-Pflücker, J. C., Maintenance of T cell specification and differentiation requires recurrent notch receptor-ligand interactions. *J. Exp. Med.* 2004. **200**: 469–479.

40 Brooker, R., Hozumi, K. and Lewis, J., Notch ligands with contrasting functions: Jagged1 and Delta1 in the mouse inner ear. *Development* 2006. **133**: 1277–1286.

41 Cheng, P., Nefedova, Y., Corzo, C. A. and Gabrilovich, D. I., Regulation of dendritic-cell differentiation by bone marrow stroma via different Notch ligands. *Blood* 2007. **109**: 507–515.

42 Santos, M. A., Sarmento, L. M., Rebelo, M., Doce, A. A., Maillard, I., Dumortier, A., Neves, H. *et al.*, Notch1 engagement by Delta-like-1 promotes differentiation of B lymphocytes to antibody-secreting cells. *Proc. Natl. Acad. Sci. USA* 2007. **104**: 15454–15459.

43 Urs, S., Roudabush, A., O'Neill, C. F., Pinz, I., Prudovsky, I., Kacer, D., Tang, Y. *et al.*, Soluble forms of the Notch Ligands Delta1 and Jagged1 promote in vivo tumorigenicity in NIH3T3 fibroblasts with distinct phenotypes. *Am. J. Pathol.* 2008. **173**: 865–878.

44 Shimizu, K., Chiba, S., Saito, T., Kumano, K. and Hirai, H., Physical interaction of Delta1, Jagged1, and Jagged2 with Notch1 and Notch3 receptors. *Biochem. Biophys. Res. Commun.* 2000. **276**: 385–389.

Full correspondence: Dr. Katsuto Hozumi, Department of Immunology, Tokai University School of Medicine, 143 Shimokasuya, Isehara, Kanagawa 259-1193, Japan
Fax: +81-463-94-2976
e-mail: hozumi@is.icc.u-tokai.ac.jp

IMMUNOLOGY ORIGINAL ARTICLE

Over-expression of Runx1 transcription factor impairs the development of thymocytes from the double-negative to double-positive stages

Won F. Wong,[1] Megumi Nakazato,[1] Toshio Watanabe,[1*] Kazuyoshi Kohu,[1] Takehiro Ogata,[1] Naomi Yoshida,[1] Yusuke Sotomaru,[2†] Mamoru Ito,[2] Kimi Araki,[3] Janice Telfer,[4] Manabu Fukumoto,[1] Daisuke Suzuki,[5] Takehito Sato,[5] Katsuto Hozumi,[5] Sonoko Habu[5] and Masanobu Satake[1]

[1]Institute of Development, Aging and Cancer, Graduate School of Life Sciences, Tohoku University, Sendai, Japan, [2]Central Laboratory for Experimental Animals, Kawasaki, Japan, [3]Institute of Embryology and Genetics, Kumamoto University, Kumamoto, Japan, [4]Department of Veterinary and Animal Sciences, Paige Laboratory, University of Massachusetts, Amherst, MA, USA, and [5]Department of Immunology, Tokai University School of Medicine, Isehara, Japan

Summary

Runx1 transcription factor is highly expressed at a CD4/CD8-double-negative (DN) stage of thymocyte development but is down-regulated when cells proceed to the double-positive (DP) stage. In the present study, we examined whether the down-regulation of Runx1 is necessary for thymocyte differentiation from the DN to DP stage. When Runx1 was artificially over-expressed in thymocytes by Lck-driven Cre, the DN3 population was unaffected, as exemplified by proper pre-T-cell receptor expression, whereas the DN4 population was perturbed as shown by the decrease in the $CD27^{hi}$ sub-fraction. In parallel, the growth rate of DN4 cells was reduced by half, as measured by bromodeoxyuridine incorporation. These events impaired the transition of DN4 cells to the DP stage, resulting in the drastic reduction of the number of DP thymocytes. The *Runx1* gene has two promoters, a proximal and a distal promoter; and, in thymocytes, endogenous Runx1 was mainly transcribed from the distal promoter. Interestingly, only distal, but not proximal, Runx1 over-expression exhibited an inhibitory effect on thymocyte differentiation, suggesting that the distal Runx1 protein may fulfil a unique function. Our collective results indicate that production of the distal Runx1 protein must be adequately down-regulated for thymocytes to transit from the DN to the DP stage, a critical step in the massive expansion of the T-cell lineage.

Keywords: double negative; double positive; Runx1; thymocyte development; transgenic mice

243

Introduction

Runx1 and Runx3 transcription factors play critical roles during thymocyte development (see ref. [1] for review). The role of each Runx protein is dependent on its expression pattern during the different stages of thymocyte differentiation. For example, Runx1 protein is produced during the CD4/CD8 double-negative (DN), CD4/CD8 double-positive (DP), CD4 single-positive (SP) and CD8 SP lineages of thymocyte differentiation.[2] Hence, *Lck*-mediated targeting of *Runx1* was reported to cause defects in the differentiation of DN thymocytes, and *CD4*-mediated targeting of *Runx1* disrupted the positive selection of CD4 SP cells.[3,4] On the other hand, Runx3 protein is produced mainly in CD8 SP thymocytes,[2,5] where it suppresses the transcription of *CD4*, a costimulatory molecule of T-cell receptors (TCRs), and that of *ThPok*, a transcription factor specifying the CD4 lineage.[6,7] Runx3 also activates the transcription of *CD8*.[2] Targeting *Runx3* resulted in the abolition of CD8 SP cells in the thymuses of targeted mice.[7]

It is worth noting that a substantial amount of Runx1 protein is expressed at the DN stage, in contrast to the Runx3 protein, which can also be detected but to a lesser extent than Runx1.[2,7,8] In accordance with its expression profile in DN cells, the targeting of *Runx3* had only a marginal effect such as a partial de-repression of CD4 expression,[7,8] whereas a *Runx1* deficiency resulted in severe defects in the differentiation of DN thymocytes. However, the observed defects varied from one report to another, namely the developmental block at either the DN1 to DN2, DN2 to DN3, or DN3 to DN4 stages of differentiation.[3,4,9] This variation may be the result of the different targeting methods used, for example, the use of different promoter-driven *Cre*-transgenic mice. In any case, the targeting studies established clearly that Runx1 is essential for the correct differentiation of DN thymocytes.

Expression of the *Runx1* gene is initiated from two distinct promoters, distal and proximal.[10,11] In thymocytes, the majority of *Runx1* transcripts represent transcription from the distal promoter.[12] Distal and proximal *Runx1* transcripts encode Runx1 proteins that are identical except for the last 19 amino acid residues (in the distal isoform) and the last five amino acids (of the proximal isoform), at the N-terminal end of the protein. Runx1 protein (mainly the distal isoform) is detected throughout the stages of thymocyte differentiation. Its level of expression is highest at the DN stage, and it is then substantially down-regulated at the DP stage.[2] This down-regulation of the Runx1 protein occurs in parallel with changes in *Runx1* transcripts.[7] The implications of this phenomenon are unknown. The studies cited above used a gene knock-out approach to evaluate the significance of Runx1 protein expression in the DN subset, but provided no explanations for the possible consequences of Runx1 down-regulation.

In the present study, we focused on the issue of whether the down-regulation of Runx1 protein is a necessary step in the correct progression of thymocytes from the DN to the DP stage. For this purpose, transgenic Runx1 was artificially over-expressed in thymocytes, with the expectation that it would disturb the physiological down-regulation of Runx1. We observed that the over-expressed Runx1 protein is an inhibitory factor during the DN to DP transition. Interestingly, this inhibitory effect was observed only with over-expression of the distal isoform, but not the proximal isoform, suggesting that this effect was unique to the distal isoform of the Runx1 transcription factor.

Materials and methods

Cell culture

The three T-cell lines EL-4, TK-1 and 1200M, and MEL cells (an erythroleukaemic cell line) were grown in RPMI-1640 medium (Gibco/Invitrogen, Carlsbad, CA), whereas NIH3T3 fibroblasts were cultured in Dulbecco's modified Eagle's medium. Both media were supplemented with 10% [volume/volume (v/v)] fetal bovine serum (FBS).

Plasmids

The plasmids *dRunx1-HA* and *pRunx1-HA* representing the murine *Runx1* coding region of the distal (d) and proximal (p) isoforms, respectively, each contained a haemagglutinin (HA) tag fused to the C-terminal of Runx1. A *Bgl*II–*Eco*RI fragment harbouring *Runx1-HA* was cleaved from each plasmid and cloned into the *Eco*RV site of the plasmid *pCAG-CAT-oligo*. This *CAT* (chloramphenicol acetyltransferase) plasmid harbours a *CAG* (chicken β-actin) promoter-driven *CAT-SV40pA* element flanked by *loxP* sites.[13] The resulting plasmids were designated as *pCAG-loxP-CAT-loxP-dRunx1-HA* and *pCAG-loxP-CAT-loxP-pRunx1-HA*, respectively.

Mice

A *Kpn*I–*Not* I fragment containing *pCAG-loxP-CAT-loxP-Runx1-HA* was purified and microinjected into fertilized eggs from C57BL/6 mice. Transgenic founders were identified and crossed to C57BL/6 mice. The presence, or absence, of the transgene was examined by polymerase chain reaction (PCR) using genomic DNA as a template. The sense and antisense primers were as follows: for *dRunx1*, 5′-ATGGCTTCAGACAGCATTTTTGAG-3′ and 5′-ATGCGTATCCCCGTAGATGCC-3′; for *pRunx1*, 5′-TCCCCCGGGCTTGGTCTGATCATC-3′ and 5′-ATGC

GTATCCCCGTAGATGCC-3′, respectively. *Proximal Lck-Cre*-transgenic mice were provided by J. Takeda.[14]

Flow cytometry

Cells were liberated from the mouse thymus and suspended in phosphate-buffered saline (PBS) containing 1% (v/v) FBS. Cell surface proteins were labelled by incubating single-cell suspensions of 2×10^6 cells with appropriately diluted monoclonal antibodies (mAbs) on ice for 30 min. Intracytoplasmic proteins were labelled by fixing and permeabilizing the surface-labelled cells using a FIX & PERM kit (Caltag Laboratories, Burlingame, CA), followed by incubation with a second mAb on ice for 30 min. The following fluorescein-conjugated mAbs were used: fluorescein isothiocyanate- (FITC-) Thy-1.2, FITC-TCR-β, FITC-CD3ε, FITC-CD25, FITC-HSA (heat stable antigen), FITC-Annexin V, phycoerythrin- (PE-) CD8a, PE-CD44, PE-CD25, PE-CD27, PE-TCR-γδ, Cychrome-CD4, Cychrome-CD8a, Cychrome-CD44 (these 14 mAbs were from BD Pharmingen, San Jose, CA), RED613-CD4 and RED613-CD8a (these two mAbs were from GibcoBRL, Gaithersburg, MD). The labelled cells were separated with an analytical EPICS-XL flow cytometer (Beckman Coulter, Miami, FL), and the data were analysed with EXPO32 software (Beckman Coulter).

Fractionation of thymocytes

Various thymocyte subsets were purified from a total thymocyte suspension using Auto-MACS (Miltenyi Biotech GmbH, Bergisch Gladbach, Germany) or FACStar (Becton Dickinson, Mountain View, CA). The subsets prepared in this way corresponded to DN1/2, DN3, DN4 and DP fractions. The DN3 was further sub-divided into DN3S and DN3L based on cell size. The purity of each isolated fraction was > 95% as judged by flow cytometry.

Immunoblot analysis

Protein was extracted from 1×10^6 cells and dissolved in 80 μl of 9 M urea, 2% (v/v) Triton-X-100, 1% [weight/volume (w/v)] dithiothreitol and 20 μl of 10% (w/v) lithium dodecylsulphate. Protein extract, equivalent to 2×10^5 cells, was loaded in one lane, separated through a sodium dodecyl sulphate 8% (w/v) polyacrylamide gel, and electroblotted on to a polyvinylidene difluoride (PVDF) membrane (BioRad, Hercules, CA). The filter was blocked by immersing it in PBS containing 5% (w/v) skimmed milk at 4° overnight. The primary antibodies used were anti-HA mAb 3F10 (Roche Diagnostics, Indianapolis, IN), anti-β-actin mAb (Santa Cruz Biotechnology, Santa Cruz, CA) or anti-panRunx-peptide rabbit serum.[15] Anti-rat immunoglobulin G or anti-rabbit immunoglobulin G were used as the secondary antibodies. Immunocomplexes were

detected using an ABC kit (Vector Laboratories, Burlingame, CA) and exposed to X-ray film (Fujifilm, Tokyo, Japan).

Southern blot analysis

Genomic DNA was prepared from the tails of mice by proteinase K digestion, phenol–chloroform extraction and ethanol precipitation. DNA was digested with *Eco*RI, electrophoresed through a 0·8% (w/v) agarose gel and processed for Southern blot analysis as described previously.[16] The hybridization probe contained the Runt domain sequence of murine *Runx1* complementary DNA (cDNA).

Reverse transcription–polymerase chain reaction analysis

RNA was extracted from cells using Isogen (Nippon Gene, Tokyo, Japan) and cDNA was synthesized from RNA using Superscript II reverse transcriptase (Invitrogen, Carlsbad, CA). The PCR amplification was performed for 25 cycles using a cDNA template and LA-*Taq* polymerase (Takara, Ohtsu, Japan). The following sense and anti-sense primers were used to detect transcripts: for *distal Runx1*, 5′–ATGGCTTCAGACAGCATTTTTGAGTC-ATTT–3′ and 5′–ACTGTCATTTTGATGGCTCTATGG-TAGGT–3′; for *proximal Runx1*, 5′–ATGCGTATCCCC-GTAGATGCCAGCAC–3′, and 5′–ACTGTCATTTTGATG-GCTCTATGGTAGGT–3′; for *β-actin*, 5′–GATGACGATA-TCGCTGCGCTG–3′ and 5′–GTACGACCAGAGGCATA-CAGG–3′; and for *pTα*, 5′-TCACACTGCTGGTAGATG-GAAGG-3′ and 5′-CATCGAGCAGAAGCAGTTTGA-3′.

Northern blot analysis

Poly(A)$^+$ RNA was selected from the RNA fraction using Oligo-dT-Latex (Takara), and 2 μg was separated on a 1% (w/v) agarose gel containing 2·2 M formaldehyde. Electronic transfer, hybridization and washing procedures were as described previously.[17] Specific *distal* or *proximal Runx1* probes corresponding to 5′ untranslated regions of each *Runx1* transcript were radioactively labelled and used for detection of each *Runx1*. Sequences of each probe were as follows: for *proximal Runx1*, 5′-CGCATCACAA CAAGCCGATTGAGTAAGGACCCTGAAAACAGCTCCTA CTAGACGGCGACAGGGGCTCGGATCTTCTGCAAGCT GCTCCCGGGAGACCAACATACAAGTTCAGAAGCCTT TATTACTACCGGAGGGGTTGTGGGGGTAGGAGACTAA ATTACCATCAGTCCCGGACTGAGATCTAGTTACACG GA&CGCATCACAACAAGCCGATTGAGTAAGGACCCT-GAAAACAGCTCCTACTAGACGGCGACAGGGGCTCGG-ATCTTCTGCAAGCTGCTCCCGGGA CGCA-3′, and for *distal Runx1*, 5′-AAACAACCACAGAACCACAAGTTGGT-AGCCTGGCAGTGTCAGAAGTGTAAGCCCAGCACAGT-GGTCAGCAGGCAGGACGAATCACACTGAATGCAAAC

51

CACAGGCTTTCGCAGAGCGGTGAAAGAAATTATAGA-
ATCCCCCGCCTTCAGGTAGTAGGTGCGTTTTCGAAA
GGAAACGATGGCTTCAGACAGCAÛAAACAACCACAG-
AACCACAAGTTGGTAGCCTGGCAGTGT-3'.

Detection of TCR-β recombination

A DN3 thymocyte subset was purified as described above, and genomic DNA was prepared from cells using Isogen. The frequency of *DJ* and/or *V(D)J* recombination was evaluated by PCR amplification using specific primers and 6·25 ng, 25 ng and 100 ng of genomic DNA as templates. The PCR cycle numbers were 28 for *Rag2*, 30 for *DJ* recombination and 33 for *V(D)J* recombination. The PCR products were separated on agarose gels and electroblotted onto PVDF membranes. The filters were processed for Southern blot hybridization using specific oligonucleotides as labelled probes. The sequences of the PCR primers and those of the oligonucleotide probes were as described previously.[18,19] Specifically, table 1 in ref. [19] is convenient to find the sequences. Recombination detected represented Dβ2-Jβ2, Vβ2-Jβ2, Vβ4-Jβ2, Vβ10-Jβ2 and Vβ14-Jβ2, respectively.

Bromodeoxyuridine labelling of cells

One milligram of 5-bromo-2-deoxyuridine (BrdU) in PBS was injected intraperitoneally into a mouse, and the thymus was excised after 4 hr. Cell surface proteins were fluorescently labelled as described above, and the cells with incorporated BrdU were then detected using a BrdU Flow Kit (BD Biosciences, San Diego, CA). Briefly, 2×10^6 cells were fixed, permeabilized, digested with 300 µg/ml DNAse I in PBS for 1 hr at 37°, and incubated with FITC-anti-BrdU for 20 min in the dark. Labelled cells were analysed by flow cytometry as described above.

Results

Expression of Runx1 transcript and protein decreases accompanying the DN to DP differentiation of thymocytes

We first examined the expression profiles of *Runx1* transcript by semi-quantitative reverse transcription (RT-) PCR analysis (Fig. 1a). The DN as well as DP fractions were prepared from thymuses of C57BL/6 mice. The DN fraction was further sub-divided into DN1/2, DN3 and DN4, using CD25 and CD44 as fractionation markers. DN3S (CD44$^-$ CD25^{hi}, small) and DN3L (CD44$^-$ CD25^{low}, large) represent sub-fractions of DN3 before and after pre-TCR mediated selection. The amount of *distal Runx1* transcript was maximal at the DN3S stage and decreased markedly at the subsequent stages such as DN3L, DN4 and DP. We note that, when primers specific
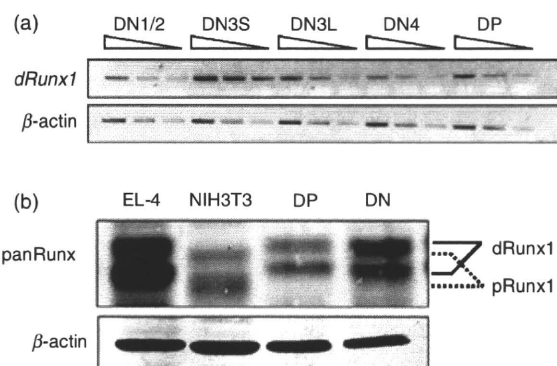

Figure 1. Expression profiles of Runx1 transcript and protein in the double-negative (DN) and double-positive (DP) fractions prepared from thymocytes of wild-type C57BL/6 mice. (a) Semi-quantitative reverse transcription–polymerase chain reaction (RT-PCR) analysis of *distal Runx1* transcript levels during thymocyte differentiation. RNA was extracted from DN1/2, DN3S, DN3L, DN4 and DP fractions each, and converted to complementary DNAs (cDNA). An increasing amount of cDNA was used for PCR as indicated. Transcript of *β-actin* served as a control. (b) Immunoblot analysis of Runx1 protein in thymocytes. Protein extracts were prepared from the DN and DP fractions as well as from EL-4 and NIH3T3 cell lines, and processed for immunoblot detection using anti-panRunx antibody. A slight but significant difference in the migration corresponded to distal and proximal Runx1 polypeptides as indicated. β-actin served as a loading control.

to proximal *Runx1* transcript were used, PCR products were detected only after extensive cycles of amplification (data not shown). This is in accordance with the literature describing scarce expression of proximal *Runx1* in thymocytes.[12]

Figure 1(b) shows immunoblot analysis of DN and DP cells, using anti-panRunx antibody. The detected doublet bands of Runx1 corresponded to unphosphorylated and phosphorylated forms, as reported.[20] In agreement with the result of the RT-PCR, the amount of Runx1 protein was higher at the DN stage and decreased at the DP stage. To confirm which of the distal and proximal Runx1 proteins was expressed in thymocytes, lysates were prepared from EL-4 and NIH3T3 cells and probed in parallel, because these cell lines expressed solely *distal* or *proximal Runx1* transcripts, respectively (Fig. S1). As expected, doublets detected for thymocytes co-migrated with doublets in EL-4 that corresponded to *distal Runx1*. Taking the above findings together, levels of *distal Runx1* transcript and protein were high at the DN stage (DN3S) and decreased at the DP stage of thymocytes.

Establishment of *Runx1*-transgenic mouse lines

The purpose of this study was to elucidate the functional significance of the Runx1 down-regulation that accompanies the differentiation of thymocytes from the DN to DP stages. We tried to counter the Runx1 down-regulation

by artificially over-expressing *distal* or *proximal Runx1* and examining its effect on thymocyte differentiation. We generated transgenic (tg) mice that harboured *pCAG-loxP-CAT-loxP-Runx1-HA* in the genome (Fig. 2a, upper). To screen for a positive mouse line, genomic DNA extracted from the tails of mice was prepared for Southern blot analysis (Fig. 2b). A probe recognizing the *Runt* domain of *Runx1* was used for detection of the transgene (indicated by arrows) as well as the endogenous gene (arrowheads). We managed to establish four lines of transgenic mice, including lines 2 and 31 harbouring *distal Runx1-tg* and lines 32 and 55 harbouring *proximal Runx1-tg*.

Runx1-HA was not expressed in *Runx1-tg* mice because the transcription of *Runx1* from the *CAG* promoter was hindered by the presence of the *CAT* gene and the *SV40*-derived poly A (pA) addition element (Fig. 2a, upper). We then crossed *Runx1-tg* mice with *Lck-Cre-tg* mice. In the T lymphocytes of *Runx1-tg;Lck-Cre-tg* double-transgenic mice, the *CAT-SV40pA* element was cleaved off by *Lck*-driven Cre recombinase, permitting the *CAG* (chicken β-actin, not *Lck*) promoter to drive the expression of *Runx1-HA* (Fig. 2a, lower part). Protein extract was prepared from the thymuses of the transgenic mice and processed for immunoblot analysis using an anti-HA antibody (Fig. 2c). *Runx1-HA*-positive bands were not detected in the single-transgenic *Runx1-tg* thymocytes (left-hand column), but were evident in the thymocytes from the *Runx1-HA-tg;Lck-Cre-tg* double-transgenic animals (right-hand column).

Essentially similar thymocyte phenotypes were obtained from the two distal mouse lines (2 and 31) and the two proximal mouse lines (32 and 55) so the results obtained from lines 2 and 32 are shown as being representative. First, an extent of Runx1 over-expression was evaluated for these two lines (Fig. 2d). The DN fractions were purified from *Lck-Cre-tg*, *distal Runx1-tg;Lck-Cre-tg* and *proximal Runx1-tg;Lck-Cre-tg* thymuses, respectively, and processed for immunoblot analyses using anti-panRunx antibody. Levels of Runx1 protein were 1·4-fold increased in both types of *Runx1-tg* cells as compared with the non-*Runx1-tg* cells. This confirmed the additive expression of transgene-derived protein.

Over-expression of *distal*, but not *proximal*, *Runx1* reduces the number of thymocytes

We observed that the macroscopic size of the thymus from *distal Runx1-tg;Lck-Cre-tg* mouse was much smaller than that from *Lck-Cre-tg* mouse (Fig. 3a). The total number of thymocytes in the *distal Runx1-tg;Lck-Cre-tg* mice (closed box) was reduced to one-ninth of that in the *Lck-Cre-tg* mice (open box), whereas the total number of thymocytes in the *proximal Runx1-tg;Lck-Cre-tg* (shaded box) was not affected ($n = 3$ for each genotype).
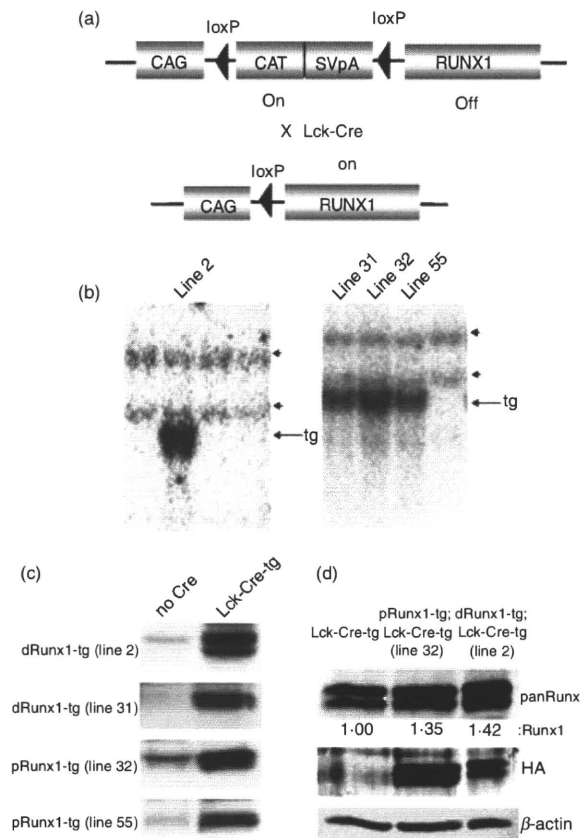

Figure 2. Establishment of *Runx1* transgenic mouse lines. (a) Schematic illustration of the *Runx1*-transgene in the mouse genome. In a *Runx1* single-transgenic mouse (upper), the *CAG* promoter-driven transcript of the *CAT* gene is polyadenylated by an *SV40pA* element, hence impeding *Runx1* expression. On the other hand, in a *Runx1* and *Cre* double-transgenic mouse (lower), the *CAT-SV40pA* element is deleted, so allowing *CAG* promoter-driven expression of *Runx1*. (b) Detection of the *Runx1*-transgene by Southern blot analysis. Genomic DNAs were prepared from each mouse line, digested by *Eco*RI and processed for Southern blot analysis using the *Runt* domain of *Runx1* as a hybridization probe. Arrows and arrowheads indicate the *Runx1* transgene and endogenous *Runx1* gene, respectively. Lines 2 and 31 harbour *distal Runx1*, whereas lines 32 and 55 harbour the *proximal Runx1* isoform. (c) Detection of transgene-derived Runx1-haemagglutinin (HA) protein by immunoblot analysis. Protein extracts were prepared from thymocytes and processed for immunoblot detection using an anti-HA antibody. The left-hand column indicated by 'no Cre' represents *Runx1* single *tg* mice, whereas the right-hand column indicated by '*Lck-Cre-tg*' represents *Runx1;Lck-Cre* double *tg* mice. dRunx1 and pRunx1 denote *distal* and *proximal* Runx1, respectively. (d) Immunoblot detection of Runx1 protein expressed in the double-negative (DN) thymocytes. The DN fractions were purified from *Lck-Cre-tg*, *distal Runx1-tg;Lck-Cre-tg* (line 2) and *proximal Runx1-tg;Lck-Cre-tg* (line 32) thymuses, respectively, and cell lysates were processed for immunoblot using anti-panRunx, anti-HA and anti-β-actin antibodies each. Levels of Runx1 protein were quantified by a densitometer, and presented as the ratios relative to that in the *Lck-Cre-tg* cells as 1.00.
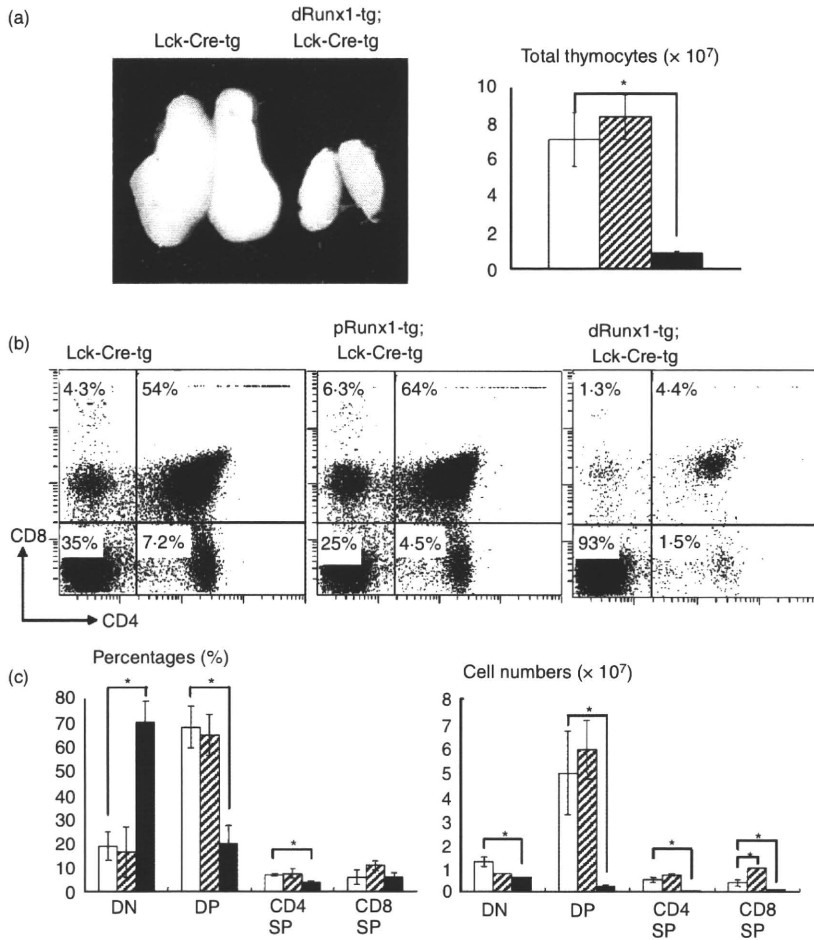
(a)

dRunx1-tg;
Lck-Cre-tg

Lck-Cre-tg

Total thymocytes (× 10⁷)

(b)

Lck-Cre-tg

pRunx1-tg;
Lck-Cre-tg

dRunx1-tg;
Lck-Cre-tg

CD8

CD4

(c)

Percentages (%)

Cell numbers (× 10⁷)

Figure 3. Effects of *Lck*-driven *Runx1* over-expression on thymocyte differentiation. (a) Gross appearance of thymuses and total numbers of thymocytes. (b) Thymocytes were isolated from the transgenic mice indicated and processed for the flow cytometric analysis of CD4 and CD8 expression. Numbers given in each quadrant indicate the percentages of cells in each subset. Representative profiles are shown here. (c) Comparison of the percentages and cell numbers of double-negative (DN), double-positive (DP), CD4 single-positive (SP) and CD8 SP subset. In (a) and (c), the genotypes of mice were *Lck-Cre-tg* (open bars), *proximal Runx1-tg;Lck-Cre-tg* (shaded bars) and *distal Runx1-tg;Lck-Cre-tg* (closed bars), respectively. Mean ± SD ($n = 3$) are shown for each thymocyte subset and each transgenic mouse. Significances of difference were statistically tested by Student's *t*-test, and if detected between the compared genotypes, they are indicated by brackets with *($P < 0.05$). (b) CD4 repression by Runx1 over-expression was not observed in the present study, unlike the case of Runx1 introduction into a thymocyte culture by retrovirus.[37] (c) The number of CD8 SP cells was significantly increased in *proximal Runx1-tg;Lck-Cre-tg* compared with *Lck-Cre-tg* thymuses ($P < 0.05$). This observation supports our previous report of *CD2*-driven, *proximal Runx1-tg* thymuses.[5]

In Fig. 3(a), statistical significance of difference was tested using Student's *t*-test, and is indicated, if any, by an asterisk ($P < 0.05$).

To examine the effect of *Runx1* over-expression, we performed flow cytometric analysis of CD4 and CD8 expression in thymocytes (Fig. 3b). As the thymocytes of *Lck-Cre-tg* mice contained an unusually high proportion of DN cells (20% on average) compared with a wild-type thymus (around 5%, data not shown), we used the *Lck-Cre-tg* mice as controls throughout this study when analysing *Runx1-tg;Lck-Cre-tg* thymuses. A remarkable difference in the DP fractions was observed between the *distal Runx1-tg;Lck-Cre-tg* and control mice. The proportion of DP cells was dramatically reduced in the *distal Runx1-tg;Lck-Cre-tg* thymus compared with the single *Lck-Cre-tg* thymus (4·4% compared to 54%). Additionally, the percentages of CD4 SP and CD8 SP cells were also significantly lower in the *distal Runx1-tg;Lck-Cre-tg* thymus (1·5% and 1·3%, respectively) compared with the *Lck-Cre-tg* thymus (7·2% and 4·3%, respectively).

From the analysis of the absolute cell counts (Fig. 3c), we found that in the *distal Runx1-tg;Lck-Cre-tg* thymus, the reduction in the total number of thymocytes (Fig. 3a)

was mainly the result of the massive reduction in the number of DP cells (Fig. 3c). Although the percentage of DN cells increased substantially in the *distal Runx1-tg;Lck-Cre-tg* thymus, the actual number of DN cells decreased to half that of the control. It is therefore likely that over-expression of *distal Runx1* impairs the DN to DP transition. In contrast to the results from *distal Runx1-tg;Lck-Cre-tg*, the percentages of each DN and DP subset were fairly similar between *proximal Runx1-tg;Lck-Cre-tg* and the control *Lck-Cre-tg* thymuses.

DN differentiation is perturbed in the *distal Runx1-tg;Lck-Cre-tg* thymocytes

To characterize the DN cells in more detail, we performed three-colour flow cytometric analysis of CD4, CD8 and Thy-1.2, and found that the ratios of Thy-1.2-positive versus Thy-1.2-negative DN cells were similar in the *Runx1-tg* and control thymuses. Furthermore, the Thy1.2⁺-gated fraction demonstrated proportions of DN, DP and SP subtypes that were essentially identical to those of non-gated thymocytes (Fig. S2). We also examined TCR-$\gamma\delta$ expression and found that the percentages of TCR-$\gamma\delta^+$
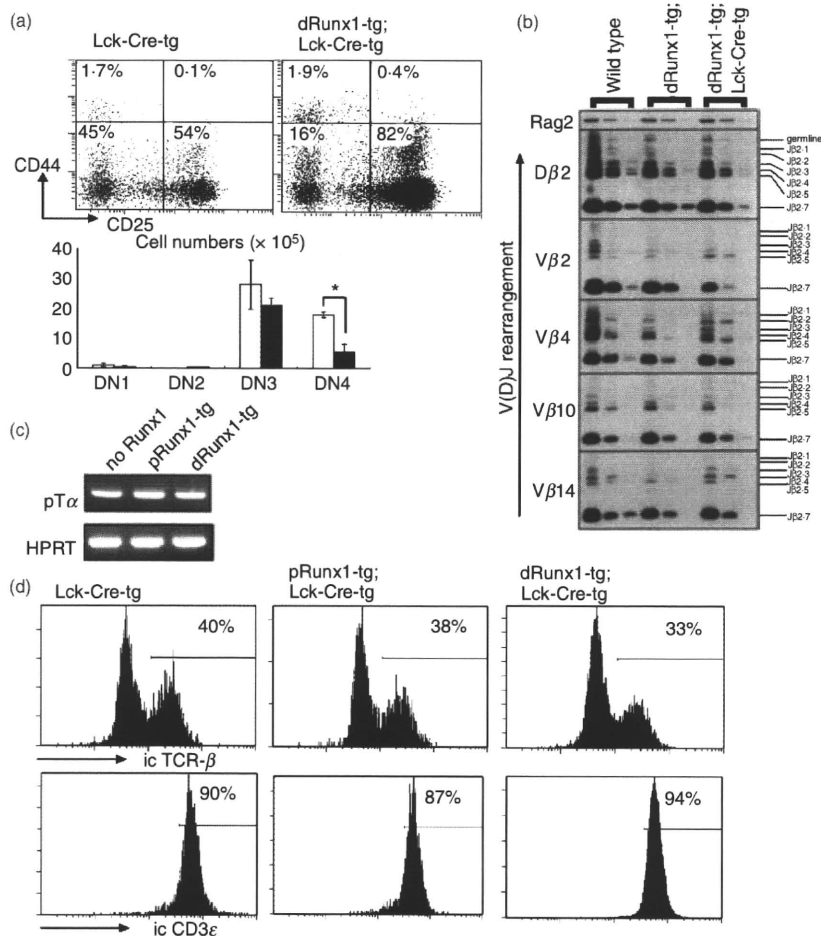
Figure 4. Effects of *Lck*-driven *Runx1* over-expression on double-negative (DN) thymocyte differentiation. (a) Sub-staging of DN thymocyte differentiation. Thymocytes from *distal Runx1-tg;Lck-Cre-tg* (closed bars) and *Lck-Cre-tg* mice (open bars) were processed for flow cytometric analysis of CD4/CD8, Thy-1.2, CD44 and CD25. The data shown here were gated for the Thy-1.2$^+$ CD4$^-$ CD8$^-$ fraction that represents authentic, DN T lymphocytes. Sub-staging of DN cells was based on the levels of CD44 and CD25 expression. The representative expression profiles are shown as well as the mean ± SD values ($n = 3$) of the absolute number of cells at each DN sub-stage. Significances of difference were statistically tested by Student's *t*-test, and if detected between the compared genotypes, they are indicated by a bracket with *($P < 0.05$). (b) Detection of *TCRβ* gene recombination in DN thymocytes. The DN3 subset of cells was purified by cell-sorting from C57BL/6 (wild-type), *distal Runx1-tg* and *distal Runx1-tg;Lck-Cre-tg* mice, and genomic DNA was prepared. Polymerase chain reaction (PCR) was performed using different amounts of template DNA and specific oligonucleotides as primers. PCR products were processed for Southern blot analysis. The patterns of *V(D)J* recombination detected are as indicated. *Rag2* served as a control. (c) Expression of *pTα* in thymocytes. RNA was prepared from total thymocytes, and processed for reverse transcription-PCR. Transcripts representing *pTα* and *HPRT* were amplified. (d) DN3 subset was purified from thymocytes, stained for intracytoplasmic T-cell receptor-*β* (TCR-*β*) and CD3ε and processed for flow cytometric analysis. Numbers indicate the proportions of TCR-*β*$^+$ and CD3ε$^+$ cells in each DN3 subset.

cells in the DN fractions were similarly low in both *Lck-Cre-tg* and *distal Runx1-tg;Lck-Cre-tg* thymuses (Fig. S3a). These results confirm that the DN cells, illustrated in Fig. 3, mostly reflect authentic T lymphocytes of αβ lineage.

The DN population can be subdivided into four substages designated as DN1 (CD44$^+$ CD25$^-$), DN2 (CD44$^+$ CD25$^+$), DN3 (CD44$^-$ CD25$^+$) and DN4 (CD44$^-$ CD25$^-$). To examine the differentiation of DN cells, we carried out four-colour flow cytometric analysis using CD4/CD8, Thy-1.2, CD44 and CD25. The CD44 and CD25 expression profiles of the Thy-1.2$^+$-gated DN fractions are shown in Fig. 4(a). In the *distal Runx1-tg;Lck-Cre-tg* thymus, the percentages of DN1 and DN2 cells were normal. However, the percentages of DN3 and DN4 cells were increased and decreased, respectively, compared with the *Lck-Cre-tg* thymus. When the absolute cell number of each DN subset was counted, the DN4, but not DN3, cell numbers were substantially decreased in the *distal Runx1-tg;Lck-Cre-tg* thymus. This suggests that over-expression of *distal Runx1* probably causes a defect at the DN4 rather than the DN3 stage.

Pre-TCR expression proceeds appropriately in the *distal Runx1-tg;Lck-Cre-tg* thymocytes

The DN3 stage is a critical step in early thymocyte differentiation as *DJ* and *V(D)J* rearrangements take place at this stage to form the pre-TCR complex.[21] Cells that fail to form a functional pre-TCR die by apoptosis. We investigated whether pre-TCR expression proceeded correctly in the *distal Runx1-tg;Lck-Cre-tg* cells. Genomic DNA was prepared from the purified DN3 fraction and used as a template for PCR amplification. Specific PCR primers and hybridization probes were designed to detect various patterns of *DJ* and *V(D)J* segment recombination.[18,19] As far as the gene combinations examined were concerned, the *DJ* and *V(D)J* segments of *TCRβ* were properly rearranged in the DN3 cells from *distal Runx1-tg;Lck-Cre-tg*, *distal Runx1-tg* and wild-type thymuses (Fig. 4b).

The expression of the pre-TCR complex itself was also examined. The major components of the pre-TCR complex include pTα, TCR-β and CD3ε. Transcripts of *pTα* were detected in thymocytes from *distal Runx1-tg;Lck-Cre-tg* mice (Fig. 4c) and intracytoplasmic TCR-β and CD3ε expression was detected by flow cytometric analysis (Fig. 4d). Both TCR-β and CD3ε were expressed to a similar extent in DN3 thymocytes from the *distal Runx1-tg;Lck-Cre-tg*, *proximal Runx1-tg;Lck-Cre-tg* and *Lck-Cre-tg* mice. Based on the observations illustrated in Fig. 4, it is not likely that over-expression of *distal Runx1* affects the process of pre-TCR expression at the DN3 stage.

DN4 differentiation as probed by CD27-expression is impaired in the *distal Runx1-tg;Lck-Cre-tg* thymocytes

We then examined the differentiation status of DN thymocytes using other markers such as HSA (Fig. 5a) and CD27 (Fig. 5b). In non-gated, *distal Runx1-tg;Lck-Cre-tg* thymocytes, a substantial peak of HSA^{hi} population was observed in addition to an HSA^{lo} population. Furthermore, mean fluorescence intensity of HSA in the DN fraction was higher in the *distal Runx1-tg;Lck-Cre-tg* compared with that in the *Lck-Cre-tg* (217 versus 122). This suggests that the majority of the *distal Runx1-tg;Lck-Cre-tg* DN cells were highly immature.

CD27 is a newly reported DN marker whose expression is low at the DN3S stage (CD27^{lo}) and increases sharply at the DN3L (CD27^{med}) and DN4 stages (CD27^{hi}).[22] Although the DN1/2 cells also express high CD27, they constitute < 3% of the entire DN population, and contribute little to the CD27$^{med/hi}$ population. These CD27^{med} and CD27^{hi} populations were substantially increased and decreased, respectively, in the DN fraction from *distal Runx1-tg;Lck-Cre-tg* thymus (43% and 57% each) compared with those from *Lck-Cre-tg* thymus (29% and 71% each). Alteration of CD27 expression pattern was analogous to the CD25 and CD44 profile in the sense that the
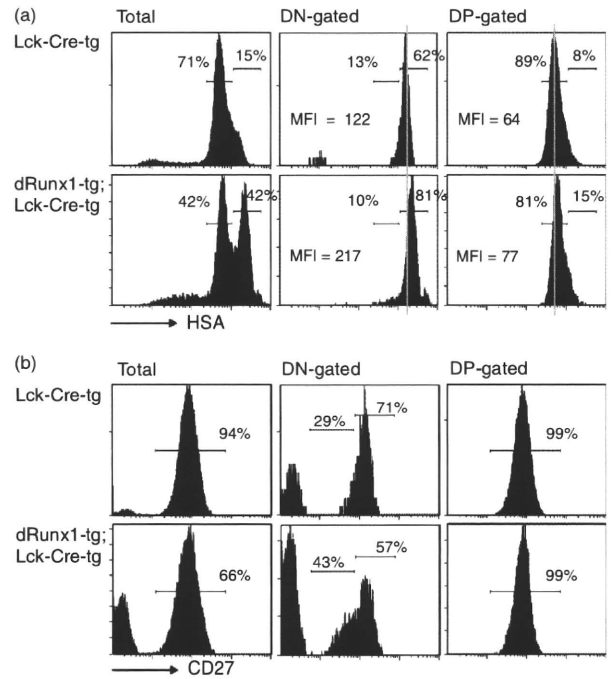

Figure 5. Flow cytometric analyses of HSA/CD27 expression in the double-negative (DN) and double-positive (DP) fractions. Thymocytes were prepared from *Lck-Cre-tg* and *distal Runx1-tg;Lck-Cre-tg* mice, and processed for flow cytometric analyses of CD4, CD8 and HSA/CD27. The DN-gated and DP-gated fractions were analysed for their fluorescence intensities of HSA (a) and CD27 (b). In (a), the percentages of HSA^{hi} and HSA^{lo} sub-fractions and the mean fluorescence intensities of HSA are indicated, whereas the numbers seen in (b) indicate the percentages of CD27$^{med/hi}$ sub-fractions. Note that the percentage of CD27$^{med/hi}$ is assumed to be 100 for the DN fractions in (b).

percentage of DN3 increased and that of DN4 decreased in the DN cells from *distal Runx1-tg;Lck-Cre-tg* thymus (see flow cytometry analyses in Fig. 4a). Collectively, the alterations of HSA and CD27 expressions observed in the *distal Runx1-tg;Lck-Cre-tg* thymocytes suggest an impairment of thymocyte differentiation at the DN3L/DN4 stage.

Over-expression of *distal Runx1* reduces the growth activity of thymocytes at the DN4 stage and impairs the DN to DP transition

As the DN4 stage was likely to be perturbed by *Runx1* over-expression, we examined the degree of cell proliferation in *Runx1-tg* thymuses. Eight-week-old mice were injected intraperitoneally with BrdU, and their thymuses were harvested after 4 hr. Thymocytes were processed for four-colour flow cytometric analysis of BrdU, CD4/8, CD25 and CD44 (Fig. 6a). For the DN2 and DN3 fractions, the percentages of BrdU$^+$ cells were comparable between the *distal Runx1-tg;Lck-Cre-tg* (closed bars) and *Lck-Cre-tg* thymocytes (open bars). However, in the DN4 cells of the *distal Runx1-tg;Lck-Cre-tg* thymus, the per-
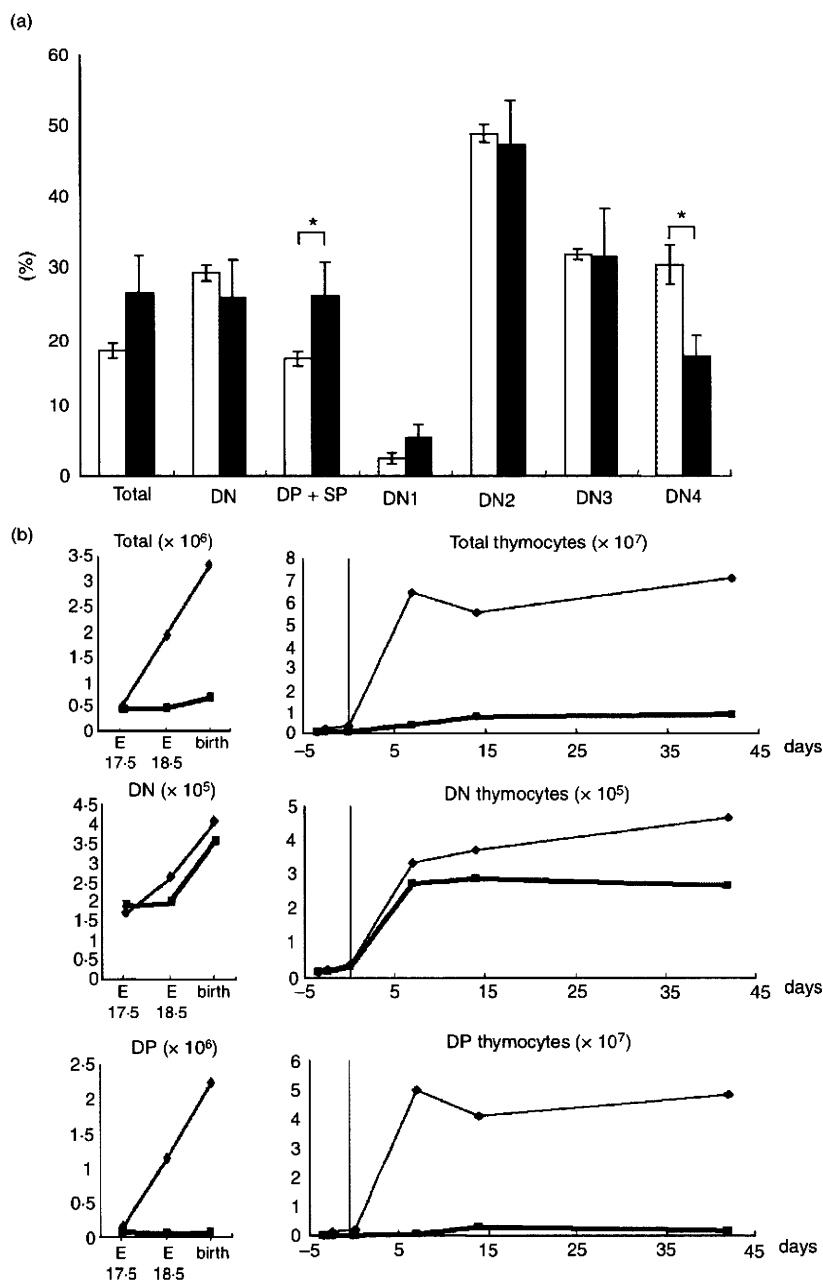
(a)

(b)

Figure 6. Effects of *Runx1-tg* on the growth and expansion of thymocytes. (a) Incorporation of bromodeoxyuridine (BrdU) into various subsets of thymocytes. *Lck-Cre-tg* mice (open boxes) and *distal Runx1-tg;Lck-Cre-tg* mice (closed boxes) were each injected with BrdU intraperitoneally. Thymocytes were prepared after 4 hr and processed for flow cytometric analysis of BrdU, CD4/CD8, CD25 and CD44. Percentages of BrdU$^+$ cells in various subsets are shown as the mean ± SD values (n = 3). Significances of difference were statistically tested by Student's t-test, and if detected between the compared genotypes, they are indicated by brackets with *($P < 0.05$). (b) Ontogeny of DN and DP thymocytes during mouse development. Thymuses were taken from mice at embryonic day 17·5 (E17.5), E18.5, at birth, 1, 2 and 6 weeks after birth, and processed for flow cytometric analysis of CD4 and CD8 expression. The numbers of total, DN and DP cells are shown in *distal Runx1-tg;Lck-Cre-tg* (thick lines) and *Lck-Cre-tg* mice (thin lines).

centage of BrdU$^+$ cells was reduced to nearly half that of the control. An increase of the BrdU$^+$ percentage in the DP + SP fraction might reflect a compensatory growth enhancement in the *distal Runx1-tg;Lck-Cre-tg* thymuses. An essentially similar result was obtained when 1-week-old mice were used for the same experiments (data not shown). We conclude therefore that over-expression of *distal Runx1* impairs the ability of DN4 thymocytes to proliferate. It must be noted that the extent of apoptosis, as measured by Annexin V staining, was not enhanced in the *distal Runx1-tg;Lck-Cre-tg* thymocytes compared with the *Lck-Cre-tg* thymocytes (Fig. S3b).

Finally, we analysed thymocyte differentiation during mouse development. Thymuses were harvested at embry-

onic day (E) 17·5, E18·5, at birth and 1, 2 and 7 weeks after birth, from *distal Runx1-tg;Lck-Cre-tg* and *Lck-Cre-tg* mice, and processed for flow cytometric analysis with CD4, CD8 and Thy-1.2. The numbers of Thy-1.2$^+$ DN and DP cells were plotted together with the development and growth of the mice (Fig. 6b). There were slightly fewer DN cells in the *distal Runx1-tg;Lck-Cre-tg* thymuses (thick line) than in the *Lck-Cre-tg* thymuses (thin line) throughout the developmental stages examined. In contrast, the number of DP cells from the *distal Runx1-tg;Lck-Cre-tg* thymuses was remarkably diminished when compared with the *Lck-Cre-tg* cells. This difference was particularly marked 1 week after birth. This was because, during this period, the total cell number (consisting mainly of DP cells) increased

dramatically in the control thymus but not in the *Runx1-tg;Lck-Cre-tg* thymus. Taken collectively, the results illustrated in Fig. 6 indicated that over-expression of *distal Runx1* appears to severely disrupt the transition of thymocytes from the DN4 to DP stages.

Discussion

Previous studies have demonstrated that the abolition of *Runx1* expression causes severe impairments in the differentiation of DN thymocytes, highlighting an indispensable role for *Runx1* at this particular stage of T-cell development.[3,4,9] These targeting studies evaluated the significance of *Runx1* expression in DN cells; however, the Runx1 protein is then down-regulated during the transition from the DN to the DP stage. In this study, we investigated whether the down-regulation of Runx1, that accompanies the DN to DP differentiation, has biological significance. This was assessed using conditional *Runx1-*transgenic mice to disrupt the down-regulation of Runx1. *Lck-Cre-*mediated deletion has been shown to be initiated at DN2 and completed by DN3.[23] Therefore, the onset of *Runx1* transgene expression can be manipulated to start at the DN2 stage by mating *Runx1-tg* mice with *Lck* promoter-driven *Cre-*transgenic mice. When *Runx1* over-expression was initiated at such an early DN stage, it resulted in a marked impairment in the transition of cells from the DN to DP stages.

The DN-cell population is not a homogeneous entity, but rather comprises a population of developing cells with different characteristics divided into four subgroups (DN1 to DN4). For example, DN1 cells retain the potential to differentiate into B-cell and myeloid lineages, but they lose/reduce this capability once they have entered the DN2 stage.[24-29] The cells at a DN3 stage undergo a critical β-selection checkpoint. In the *distal Runx1-tg;Lck-Cre-tg* DN3 thymocytes, rearrangement of the *TCRβ* locus and pre-TCR expression did not appear to be affected.

On the other hand, in the same *distal Runx1-tg;Lck-Cre-tg* thymuses, the number of DN4 cells was substantially decreased, and the proportion of CD27^hi (DN4) population was remarkably reduced. In parallel, an extent of cell growth, as measured by BrdU incorporation, was decreased by nearly half in these double-transgenic DN4 cells. Hence, the differentiation of *distal Runx1-tg;Lck-Cre-tg* thymocytes was probably perturbed during the DN4 stage and/or the DN4 to DP transition. The DN to DP transition is the step when cells rapidly undergo massive expansion as seen in the thymocyte ontogeny. Disruption in the normal processing of this transition is a likely explanation for the paucity of DP cells in *distal Runx1-tg;Lck-Cre-tg* thymuses (for example, if the normal growth rate decreased by half during each of four cell divisions, the resulting cell number would be one-sixteenth that of the *Lck-Cre-tg* control thymus).

In this study we have shown that the over-expression of *distal Runx1* is deleterious for the DN4 thymocytes. In contrast, *vav-*promoter driven, over-expression of *distal Runx1* is reported to be oncogenic in the T-cell lineage and to cause lymphoma in mice.[30,31] A clue for the apparently discrepant effects of Runx1 over-expression on thymocytes might be found in a study of *CD2-Runx2-tg* thymuses by Vaillant *et al.*[32] There, as in the present study, Runx2 over-expression causes anti-proliferative effects and a differentiation block at the DN to DP intermediate stage, but, unlike the present case, simultaneously and eventually brings about predisposition to lymphoma development. On the other hand, we previously reported that cell division in *TCR* and *Runt* (a dominant interfering form of *Runx1*) double-transgenic thymocytes was also moderately impaired during the DN4 to DP transition.[33] Considering together the previous reports and the present results, for the cells to pass safely through the critical DN4 point, a dosage of Runx1 must be adequately regulated within a rather narrow window.

The transcription of the *Runx1* gene is initiated either from the distal or proximal promoters.[10,11] This feature is conserved in all vertebrate *Runx* genes examined, and it is shared by all three members of the *Runx* gene family (Runx1, Runx2 and Runx3). The distal and proximal Runx1 proteins are identical to each other, except for the extreme N-terminal 19 (distal) and five (proximal) amino acid residues. Hence, the abolition of DP thymocytes by the over-expression of *distal Runx1*, but not *proximal Runx1*, can be ascribed solely to the differences in the N-termini of the two Runx1 isoforms. In fact, the distal Runx1 protein binds to a Runx consensus binding site with a two-fold to three-fold higher affinity than does the proximal Runx1 protein.[12] In addition, the distal and proximal forms of the Runx3 protein exhibit different activities in assays using Runx site-dependent reporter plasmids, in which only the N-terminal region of the distal, but not the proximal, Runx3 protein possesses transactivation capability.[34] Furthermore, the selective loss or transgenic over-expression of the proximal or distal Runx2 isoforms have been shown to cause differential effects on bone development in mice.[35,36] It is conceivable that the 19 amino acids of distal Runx1 (highly conserved with Runx2/3) also possess a unique transcriptional modulating activity, which influences DN-cell differentiation. It must be noted that the major species of Runx1 expressed and/or down-regulated in the thymus is a distal Runx1. This observation is in concordance with our observation that over-expression of distal, but not proximal, *Runx1* catastrophically impaired DN-cell development.

Acknowledgements

58

providing us with *Lck-Cre*-transgenic mice. This work was supported in part by a research grant from the Japan Science and Technology. M.S. is a participant in the Global COE Program 'Network Medicine' at Tohoku University.

Disclosures

References

1 Kohu K, Kubo M, Ichikawa H, Ohno S, Habu S, Sato T, Satake M. Pleitropic roles of Runx transcription factors in the differentiation and function of T lymphocytes. *Curr Immunol Rev* 2008; 4:101–15.

2 Sato T, Ohno S, Hayashi T, Sato C, Kohu K, Satake M, Habu S. Dual functions of Runx proteins for reactivating CD8 and silencing CD4 at the commitment process into CD8 thymocytes. *Immunity* 2005; 22:317–28.

3 Egawa T, Tillman RE, Naoe Y, Taniuchi I, Littman DR. The role of the Runx transcription factors in thymocyte differentiation and in homeostasis of naive T cells. *J Exp Med* 2007; 204:1945–57.

4 Ichikawa M, Asai T, Saito T et al. AML-1 is required for megakaryocytic maturation and lymphocytic differentiation, but not for maintenance of hematopoietic stem cells in adult hematopoiesis. *Nat Med* 2004; 10:299–304.

5 Hayashi K, Abe N, Watanabe T, Obinata M, Ito M, Sato T, Habu S, Satake M. Overexpression of AML1 transcription factor drives thymocytes into the CD8 single-positive lineage. *J Immunol* 2001; 167:4957–65.

6 Setoguchi R, Tachibana M, Naoe Y, Muroi S, Akiyama K, Tezuka C, Okuda T, Taniuchi I. Repression of the transcription factor Th-POK by Runx complexes in cytotoxic T cell development. *Science* 2008; 319:822–5.

7 Taniuchi I, Osato M, Egawa T, Sunshine MJ, Bae SC, Komori T, Ito Y, Littman DR. Differential requirements for Runx proteins in CD4 repression and epigenetic silencing during T lymphocyte development. *Cell* 2002; 111:621–33.

8 Woolf E, Xiao C, Fainaru O et al. Runx3 and Runx1 are required for CD8 T cell development during thymopoiesis. *Proc Natl Acad Sci USA* 2003; 100:7731–6.

9 Talebian L, Li Z, Guo Y et al. T-lymphoid, megakaryocyte, and granulocyte development are sensitive to decreases in CBFβ dosage. *Blood* 2007; 109:11–21.

10 Ghozi MC, Bernstein Y, Negreanu V, Levanon D, Groner Y. Expression of the human acute myeloid leukemia gene AML1 is regulated by two promoter regions. *Proc Natl Acad Sci USA* 1996; 93:1935–40.

11 Levanon D, Groner Y. Structure and regulated expression of mammalian *RUNX* genes. *Oncogene* 2004; 23:4211–9.

12 Telfer JC, Rothenberg EV. Expression and function of a stem cell promoter for the murine *CBFalpha2* gene: distinct roles and regulation in natural killer and T cell development. *Dev Biol* 2001; 229:363–82.

13 Araki K, Araki M, Miyazaki J, Vassalli P. Site-specific recombination of a transgene in fertilized eggs by transient expression of Cre recombinase. *Proc Natl Acad Sci USA* 1995; 92:160–4.

14 Takahama Y, Ohishi K, Tokoro Y, Sugawara T, Yoshimura Y, Okabe M, Kinoshita T, Takeda J. Functional competence of T cells in the absence of glycosylphosphatidylinositol-anchored proteins caused by T cell-specific disruption of the *Pig-a* gene. *Eur J Immunol* 1998; 28:2159–66.

15 Kanto S, Chiba N, Tanaka Y et al. The PEBP2β/CBFβ-SMMHC chimeric protein is localized both in the cell membrane and nuclear subfractions of leukemic cells carrying chromosomal inversion 16. *Leukemia* 2000; 14:1253–9.

16 Okada H, Watanabe T, Niki M et al. AML1⁻/⁻ embryos do not express certain hematopoiesis-related gene transcripts including those of the PU.1 gene. *Oncogene* 1998; 17:2287–93.

17 Chiba N, Watanabe T, Nomura S, Tanaka Y, Minowa M, Niki M, Kanamaru R, Satake M. Differentiation dependent expression and distinct subcellular localization of the protooncogene product, PEBP2β/CBFβ, in muscle development. *Oncogene* 1997; 14:2543–52.

18 Senoo M, Wang L, Suzuki D, Takeda N, Shinkai Y, Habu S. Increase of TCR Vβ accessibility within Eβ regulatory region influences its recombination frequency but not allelic exclusion. *J Immunol* 2003; 171:829–35.

19 Suzuki D, Wang L, Senoo M, Habu S. The positional effect of Eβ on Vβ genes of TCRβ chain in the ordered rearrangement and allelic exclusion. *Int Immunol* 2005; 17:1553–60.

20 Tanaka T, Kurokawa M, Ueki K et al. The extracellular signal-regulated kinase pathway phosphorylates AML1, an acute myeloid leukemia gene product, and potentially regulates its transactivation ability. *Mol Cell Biol* 1996; 16:3967–79.

21 von Boehmer H, Aifantis I, Feinberg J, Lechner O, Saint-Ruf C, Walter U, Buer J, Azogui O. Pleiotropic changes controlled by the pre-T-cell receptor. *Curr Opin Immunol* 1999; 11:135–42.

22 Taghon T, Yui MA, Pant R, Diamond RA, Rothenberg EV. Developmental and molecular characterization of emerging β- and γδ-selected pre-T cells in the adult mouse thymus. *Immunity* 2006; 24:53–64.

23 Wolfer A, Wilson A, Nemir M, MacDonald HR, Radtke F. Inactivation of Notch1 impairs VDJβ rearrangement and allows pre-TCR-independent survival of early αβ lineage thymocytes. *Immunity* 2002; 16:869–79.

24 Bell JJ, Bhandoola A. The earliest thymic progenitors for T cells possess myeloid lineage potential. *Nature* 2008; 452:764–7.

25 Porritt HE, Rumfelt LL, Tabrizifard S, Schmitt TM, Zuniga-Pflucker JC, Petrie HT. Heterogeneity among DN1 prothymocytes reveals multiple progenitors with different capacities to generate T cell and non-T cell lineages. *Immunity* 2004; 20:735–45.

26 Rothenberg EV. Cell lineage regulators in B and T cell development. *Nat Immunol* 2007; 8:441–4.

27 Rothenberg EV, Moore JE, Yui MA. Launching the T-cell-lineage developmental programme. *Nat Rev Immunol* 2008; 8:9–21.

28 Schmitt TM, Ciofani M, Petrie HT, Zuniga-Pflucker JC. Maintenance of T cell specification and differentiation requires recurrent notch receptor–ligand interactions. *J Exp Med* 2004; 200:469–79.

29 Wada H, Masuda K, Satoh R, Kakugawa K, Ikawa T, Katsura Y, Kawamoto H. Adult T-cell progenitors retain myeloid potential. *Nature* 2008; 452:768–72.

30 Blyth K, Slater N, Hanlon L, Bell M, Mackay N, Stewart M, Neil JC, Cameron ER. Runx1 promotes B-cell survival and lymphoma development. *Blood Cells Mol Dis* 2009; 43:12–9.

31 Wotton S, Stewart M, Blyth K, Valliant F, Kilbey A, Neil JC, Cameron ER. Proviral insertion indicates a dominant oncogenic role for Runx1/AML-1 in T-cell lymphoma. *Cancer Res* 2002; 62:7181–5.

32 Vaillant F, Blyth K, Andrew L, Neil JC, Cameron ER. Enforced expression of Runx2 perturbs T cell development at a stage coincident with β-selection. *J Immunol* 2002; 169:2866–74.

33 Sato T, Ito R, Nunomura S, Ohno S, Hayashi K, Satake M, Habu S. Requirement of transcription factor AML1 in proliferation of developing thymocytes. *Immunol Lett* 2003; 89:39–46.

34 Chung DD, Honda K, Cafuir L, McDuffie M, Wotton D. The Runx3 distal transcript encodes an additional transcriptional activation domain. *FEBS J* 2007; 274:3429–39.

35 Kanatani N, Fujita T, Fukuyama R et al. Cbf β regulates Runx2 function isoform-dependently in postnatal bone development. *Dev Biol* 2006; 296:48–61.

36 Xiao Z, Awad HA, Liu S, Mahlios J, Zhang S, Guilak F, Mayo MS, Quarles LD. Selective Runx2-II deficiency leads to low-turnover osteopenia in adult mice. *Dev Biol* 2005; 283:345–56.

37 Telfer JC, Hedblom EE, Anderson MK, Laurent MN, Rothenberg EV. Localization of the domains in Runx transcription factors required for the repression of CD4 in thymocytes. *J Immunol* 2004; 172:4359–70.

Supporting Information

Additional Supporting information may be found in the online version of this article:

Figure S1. Northern blot analysis *of Runx1* transcripts in various mouse cell lines.

Figure S2. (a) Total numbers of Thy-1.2⁺ gated thymocytes. (b) Comparison of the percentages and cell numbers of Thy-1.2⁺ gated DN, DP, CD4 SP and CD8 SP subsets.

Figure S3. Expression profiles of TCR-γδ and Annexin-V in the DN and DP cells from *distal Runx1-tg;Lckl-Cre-tg* and *Lck-Cre-tg* thymi.

Please note: Wiley-Blackwell are not responsible for the content or functionality of any supporting materials supplied by the authors. Any queries (other than missing material) should be directed to the corresponding author for the article.

59

Original Paper

Th2 Immune Response Plays a Critical Role in the Development of Nickel-Induced Allergic Contact Dermatitis

Shiro Niiyama[a] Hidekazu Tamauchi[b] Yasuyuki Amoh[a] Masazumi Terashima[c]
Yukiko Matsumura[d] Maho Kanoh[a] Sonoko Habu[e] Jun Komotori[d]
Kensei Katsuoka[a]

Departments of [a]Dermatology and [b]Microbiology, Kitasato University School of Medicine, Sagamihara,
[c]Manufacturing Ehime Plant, Dainippon Sumitomo Pharma Co. Ltd., Nishihama, [d]Department of Mechanical
Engineering, Keio University, Yokohama, and [e]Division of Host Defense Mechanism, Department of Immunology,
Tokai University School of Medicine, Isehara, Japan

Abstract
Background: The precise roles of T helper (Th)1-type and Th2-type cytokine responses in nickel (Ni)-induced allergic contact dermatitis have not yet been clearly defined. We investigated the involvement of Th2 cytokines in Ni-induced contact hypersensitivity reaction using GATA-3 transgenic (Tg) mice. **Methods:** A Ni-titanium (Ti) alloy was implanted under the skin of GATA-3 Tg mice. A Ni solution was then injected 1 month after sensitization. The ear swelling response was measured at several time points after the injection; the cytokine levels in the skin were measured at 48 h after injection, and the serum levels of IgE were measured 1 month after injection. In addition, purified CD4+ splenic cells obtained from the GATA-3 Tg mice sensitized with the Ni-Ti alloy were infused into Rag-2$^{-/-}$ mice, and the ear swelling response of these mice after a further challenge with Ni solution was also measured. **Results:** Marked ear swelling and elevated serum IgE levels and skin tissue levels of IL-4 were observed in Ni-Ti-sensitized GATA-3 Tg mice. The Rag-2$^{-/-}$ mice transfused with the CD4+ splenic cells from the Ni-Ti

alloy sensitized GATA-3 Tg mice showed a significantly more pronounced ear swelling response than the control mice. **Conclusion:** We confirmed the participation of Th2-type immune reactions in Ni-induced allergy using GATA-3 Tg mice.

Copyright © 2010 S. Karger AG, Basel

Introduction

A variety of metals are known to be present in the environment; in recent years, allergic contact dermatitis (ACD) caused by these metals has drawn attention. The use of nickel (Ni), in particular, in numerous industrial processes, such as Ni plating and the production of Ni alloys, provides numerous opportunities for sensitization, and the reported sharp increase in Ni allergy has become a serious cause for concern. Ni-induced ACD has been reported to be a delayed-type hypersensitivity reaction associated with a T cell-mediated response following the exposure of skin to metal [1]. It has been estimated that about 4–8% of all males and 18–30% of all females in the industrialized world are sensitized to Ni [2–4]. Ni-induced ACD involves the activation of Ni-specific T cells, followed by the proliferation and induction of cytokine

Correspondence to: Dr. Hidekazu Tamauchi
Department of Microbiology
Kitasato University School of Medicine
1-15-1 Kitasato, Minami, Sagamihara, Kanagawa 253-0374 (Japan)
Tel. +81 42 778 8558, Fax +81 42 778 8441, E-Mail hidetama@med.kitasato-u.ac.jp

production [5]. Earlier studies suggested that the delayed-type hypersensitivity reaction to Ni in humans predominantly involved interferon (IFN)-γ-producing T cells [6–8], but subsequent studies of Ni-specific T cell clones have shown the involvement of mixed T helper (Th)1- and Th2-type cytokine responses in this condition [9, 10]. Moreover, Yokozeki et al. [11] described a murine model of contact sensitization to paraphenylenediamine (PPD) induced by the application of PPD to mouse skin and demonstrated that Th2-like γδT cells played a role in the development of the ACD in response to exposure to PPD. However, the association between the Th1- and Th2-type cytokine responses involved in the development of ACD in vivo has not yet been clearly defined.

GATA-3 is selectively expressed in the T cell lineage from the early stage of the development of the thymus [12, 13]. Among mature peripheral T cells, a low level of GATA-3 expression is observed in CD4+ naive T cells, and while the expression increases in Th2 cells during the process of their differentiation in vivo, the Th1 cells do not express this gene [14, 15]. The exclusive expression of GATA-3 in Th2 cells is thought to play an important role in Th2-specific functions and/or cytokine gene expressions [16]. In vitro studies have demonstrated that the ectopic overexpression of GATA-3 in cell lines results in an increase in the products of Th2 cytokine genes or the enhancement of their promoter activities [17, 18]. We previously demonstrated that the exposure of actively sensitized lck-GATA-3-transgenic (GATA-3 Tg) mice to ovalbumin aerosol increased the expression of both interleukin (IL)-5 and IL-13, the number of eosinophils in the bronchoalveolar lavage fluid, and the serum IgE levels [19]. In the present study, we investigated the immune reactions involved in the ACD response to Ni in GATA-3 Tg mice, and our results suggested that Th2-type immune reactions might play an important role in Ni-induced contact hypersensitivity reactions.

Materials and Methods

Animals

Murine GATA-3 cDNA in pBlueScript SK was provided by Dr. M. Yamamoto (Tsukuba University School of Medicine, Tsukuba, Japan). Transgenic mice harboring GATA-3 have been described previously [19]. All animals were housed under specific-pathogen-free conditions and had free access to a commercial diet and water. In this study, the animals were used at 8–15 weeks of age. Each experimental group consisted of at least 5 mice. All experiments were conducted in accordance with the Guidelines for Animal Experimentation published by the Japanese Association for Laboratory Animal Science (1987).

Contact-Sensitizing Agent

Ni-titanium (Ti) alloy bars (Ni-49.2 %Ti) were cut into sections 5 mm in diameter and 3 mm thick. The sections were then ground and polished to an ash surface and ultrasonically cleaned with acetone and ethanol. The Ni-Ti alloy test pieces were prepared using isothermal oxidation treatment. Briefly, the polished samples were heated in a furnace under a flow of 16 ml/min nitrogen and 4 ml/min oxygen and kept at 500°C (#500) for 30 min, then cooled to room temperature.

Induction of Contact Hypersensitivity to Ni

For the implantation of the test pieces, the GATA-3 Tg mice and their wild-type (WT) littermate controls (C57/BL6 mice) were anesthetized, and the coat on their backs was shaved. Part of the exposed skin was incised, the test piece was implanted under the skin, and the wound was closed with surgical clips.

Challenge and Measurement

One month after the implantation of the test piece, 10 μl of an aqueous Ni solution [Wako Nickel Std. Soln. Ni(NO$_3$)$_2$ in 0.1 mol/l · HNO$_3$; Lot No. YPK9895] that had been purchased from Wako Pure Chemical Industries Ltd. was injected into the skin of the left pinna of the GATA-3 Tg mice and WT mice, and saline was injected into the skin of the right pinna.

To determine the time course of the changes in the ear-swelling responses, the ear skin thickness on either side was measured at 1, 3, 24, 48 and 72 h and at 3, 7, 14 and 28 days after the challenge using an engineer's micrometer (Peacock, Ozaki Engineering, Tokyo, Japan); then, the difference in the thickness of the two ears was calculated for each time point.

Measurement of the Serum Concentrations of IgE, IgG1 and IgG2a

The total serum levels of IgE, IgG1 and IgG2a antibody in the sensitized/challenged mice were measured using sandwich enzyme-linked immunosorbent assays (ELISA). Serial dilutions of the test sera and control sera were incubated in 96-well microplates coated with anti-mouse antibody directed against each isotype. Biotin-labeled rat antibody against mouse IgE, IgG1 and IgG2a was added before the second incubation. After a thorough washing, the plates were incubated with streptavidin-horseradish peroxidase (HRP); the color that developed during a eroxidase reaction in TMB 3, 3′, 5, 5′-tetramethylbenzidine substrate was measured at 450 nm using an ELISA plate reader.

Quantification of the Cytokine Levels in the Supernatants of the Skin Tissue Extracts

Extracts from the ear lobe tissue were prepared for ELISA as described by Ferguson et al. [20]. Briefly, the ears were excised at 48 h after Ni application and were immediately homogenized with 500 μl of 0.1% Tween 20 in phosphate-buffered saline (PBS). The samples were quickly frozen in liquid nitrogen, thawed in a 37°C water bath, sonicated for 15 s, and sedimented by centrifugation for 5 min at 13,000 g. The supernatants were stored at –80°C before the cytokine assays. The ELISAs for IL-4, IL-5 and IFN-γ were performed using the respective ELISA kits (Endogen Inc., Woburn, Mass., USA). The IL-13 assay was conducted using the mouse IL-13 Quantikine ELISA kit (R&D Systems, Minneapolis, Minn., USA) in accordance with the manufacturer's instructions.

304   Int Arch Allergy Immunol 2010;153:303–314   Niiyama et al.

61

Histological Examination

The ear skin specimens were excised and fixed in 10% formalin, then processed and stained with hematoxylin and eosin or toluidine blue. The numbers of mononuclear cells, neutrophils and eosinophils infiltrating the dermis were counted in using micrometer sections of tissue specimens stained with hematoxylin and eosin. The number of mast cells infiltrating the dermis was evaluated by staining sections of the tissue specimens with toluidine blue solution, and the tissue sections were examined at a magnification of ×400. At least 10 fields were examined per ear lobe. The number of cells was counted and expressed as the number of cells per square millimeter area.

Passive Transfer of the Contact Hypersensitivity Reaction

To determine the effect of purified CD4+ T cells isolated from the GATA-3 Tg mice on the development of the contact hypersensitivity reaction, the GATA-3 Tg mice and WT mice were sensitized with the Ni-Ti alloy and the spleen cells were isolated on day 30. A single-cell suspension was then prepared by gentle teasing; the suspension was washed 3 times with PBS, and the washed cells were passed through a column packed with nylon fibers (Wako Pure Chemicals, Osaka, Japan). CD4+ T cells were positively selected using magnetic sorting with Dynabeads and DTACHa-BEAD mouse CD4. The CD4+ T cell specimens were usually >95% pure according to a flow cytometry analysis. The CD4+ T cells (2×10^6/mouse) were intravenously infused into Rag-2$^{-/-}$ mice. The ears of the recipient mice were immediately challenged with Ni solution, and the ear swelling response was measured at 0.5, 1, 3, 24, 48 and 72 h after the challenge.

Indirect Immunohistochemical Staining

Indirect immunohistochemical staining was performed on 5-μm-thick frozen sections of the ear lobe skin. After they were thawed, the sections were air-dried for 1 h and then fixed with cold acetone for 10 min. Endogenous peroxidase activity was blocked by treatment with 3% hydrogen peroxide for 5 min at room temperature, and the slides were incubated with 5% fetal calf serum in PBS overnight at 4°C to block nonspecific protein binding. The slides were then incubated with anti-mouse CD4 (1:100; Bio Legend, San Diego, Calif., USA) for 60 min at room temperature, washed with PBS, and incubated with biotinylated rabbit anti-rat IgG (1:400; Dako, Glostrup, Denmark) for 15 min at room temperature. After the slides were washed with PBS, they were incubated with HRP-conjugated streptavidin solution (Dako) for 10 min at room temperature. Finally, immunoreactivity was visualized by staining with 8-amino-9-ethylcarbazole solution (Dako) and counterstaining with Mayer's hematoxylin (Wako Pure Chemical).

Ear Swelling Response in GATA-3 Tg Mice Implanted with the Ni-Ti (#500) Test Piece and Measurement of the Serum IgE Concentration

The Ni-Ti test pieces were subjected to oxygen diffusion processing and implanted subcutaneously in the mice. One month later, the ear skin of the mice was injected with Ni solution, and the ear swelling response was measured using a thickness gauge. The serum IgE antibody levels were measured one month later using an ELISA.

Examination of Ni Ion Elution from the Oxygen Diffusion Processed Ni-Ti Alloy Subjected to Oxygen Diffusion Processing

The test pieces subjected to oxygen diffusion processing were soaked in 3% sodium chloride (NaCl) solution at 37°C for 28 days, and the density of the Ni ions eluted into the solution was measured using atomic absorption photometry. The surface area of the test piece was assumed to be 113 mm^2, and the volume of the solution used to measure the Ni ion density was 5 ml.

Statistical Analysis

The experimental data were expressed as the mean ± standard deviation (SD). The statistical significance of differences in the data was determined using a Student t test. $p < 0.05$ was considered to denote significance.

Results

Increased Ear Swelling Response to Ni Challenge in GATA-3 Tg Mice Implanted with Ni-Ti Alloy

The GATA-3 Tg and WT mice were sensitized with a Ni-Ti alloy to evaluate the ability of the GATA-3 Tg mice to mount a Ni-induced ACD reaction. A significantly greater amount of swelling was recognized in the GATA-3 Tg mice than in the WT mice until 4 days after the Ni antigen challenge. Thereafter, however, the extent of the swelling was almost the same in both the GATA-3 Tg and WT mice. The reactions within 1 h after the local injection of Ni solution were considered to represent a physical response to the local injection, since no differences in the reactions between the GATA-3 Tg mice and WT mice were observed. The characteristics of the specific responses seen subsequently in the GATA-3 Tg mice suggested that Th2-type immune reactions were involved in the reactions. Also, as reported previously, the reactions that were observed from 4 days onward after the Ni antigen challenge were considered to represent Th1-type immune reactions. The ear swelling reactions occurring after the local injection of Ni solution into the non Ni-Ti alloy sensitized mice averaged 1–5 × 0.01 mm (data not shown). The values were the same in the GATA-3 Tg mice and WT mice at every time-point (fig. 1). The reaction of GATA-3 Tg mice and WT mice not sensitized to the Ni-Ti alloy test piece to a challenge with 10 μl of HNO$_3$ solution was almost the same as that following the administration of saline (data not shown).

Serum IgE Elevation in GATA-3 Tg Mice Challenged with Ni

IgE is known to play an important role in the pathogenesis of ACD [21, 22]. GATA-3 Tg mice and WT mice
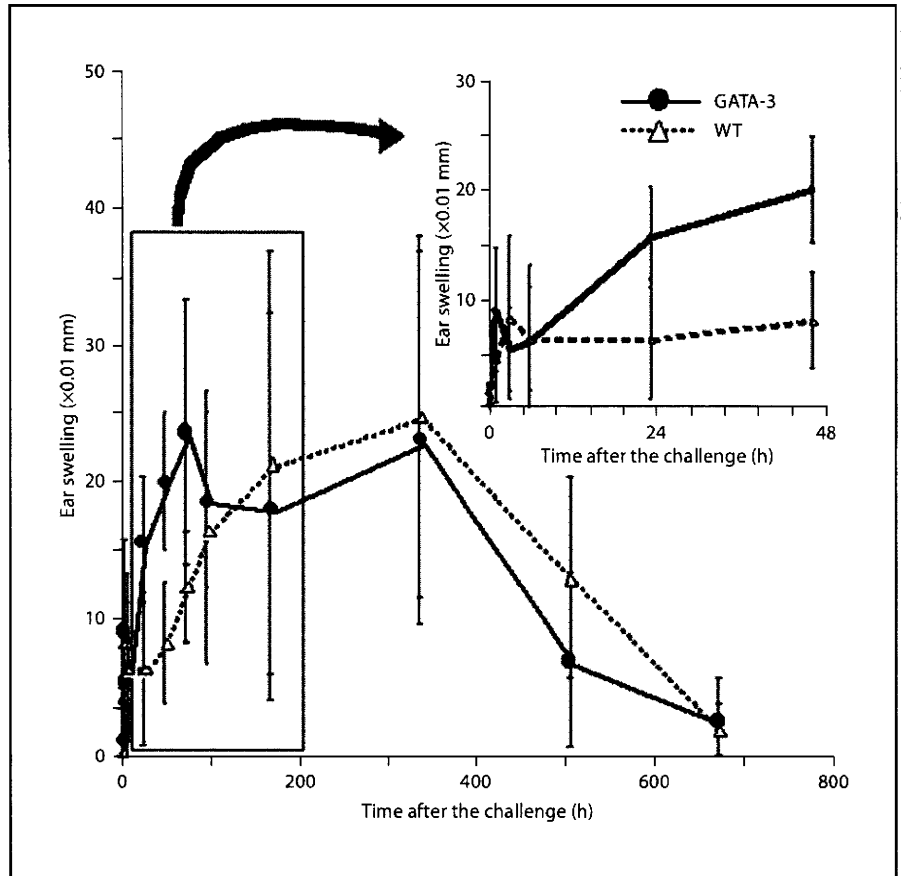
Fig. 1. GATA-3 Tg mice exhibit enhanced allergic contact dermatitis. The ear skin thickness of the Ni-sensitized GATA-3 Tg and the WT mice was measured at the time points indicated after the subcutaneous injection of 10 μl of a solution of Ni (1,000 ppm) into the left ear and 10 μl of saline into the right ear. The differences in the thickness between the right and left ears after the challenge are shown. The data are the means ± SD of 5 animals per group and are representative of 3 independent experiments. $p < 0.05$ vs. WT mice.

were sensitized with Ni and then challenged with Ni or saline. Twenty-eight days after the Ni challenge, the serum concentrations of IgE, IgG1, and IgG2a were measured using ELISA. Neither the nonsensitized/challenged nor the nonsensitized/nonchallenged mice showed any detectable IgE in their sera (data not shown). The Ni-Ti alloy sensitized/Ni-challenged GATA-3 Tg mice showed significantly higher serum IgE concentrations than the Ni-Ti alloy sensitized/Ni-challenged WT mice (fig. 2a). On the other hand, the serum concentrations of IgG1 and IgG2a were comparable in the Ni-Ti alloy sensitized/Ni-challenged GATA-3 Tg and WT mice in this experiment (fig. 2a).

Cytokine Production in the Ear Tissue of the Ni-Challenged GATA-3 Tg Mice

The measurement of IL-4 in the supernatant obtained from the skin tissue of the Ni-Ti alloy sensitized/Ni-challenged GATA-3 Tg mice and WT mice revealed significantly higher levels of the cytokine in the ear-tissue supernatant obtained from the Ni-Ti alloy sensitized/Ni-

challenged GATA-3 Tg mice (fig. 2b). The extracts were prepared using samples from the ears of the Ni-challenged GATA-3 Tg or WT mice obtained 30 days after the implantation of the Ni-Ti alloy. The IL-4 level in the Ni-Ti alloy sensitized/Ni-challenged GATA-3 Tg mice was twice as high as that in the control WT mice. In contrast, no changes in the levels of IL-5 or IL-13 were observed in the ear-tissue supernatant of either the Ni-Ti alloy sensitized/Ni-challenged GATA-3 Tg or WT mice (fig. 2b), although the IFN-γ levels were significantly lower in the Ni-Ti alloy sensitized/Ni-challenged GATA-3 Tg mice than in the Ni-Ti alloy sensitized/Ni-challenged WT mice (fig. 2b).

Histopathology of the Ni-Induced Contact Hypersensitivity Reaction in GATA-3 Tg Mice

Since the ACD to Ni in the GATA-3 Tg mice increased at 48–72 h after the challenge, we histologically examined the ear skin of the GATA-3 Tg and WT mice sensitized with the Ni-Ti alloy. The results showed severe edema in the challenged skin of the GATA-3 Tg mice (fig. 3a), but

63